June, 1979

Adaptive nonlinear image restoration by a modified Kalman filtering approach

Sarah A. Rajala, *Rice University*

RICE UNIVERSITY

ADAPTIVE NONLINEAR IMAGE RESTORATION BY A
MODIFIED KALMAN FILTERING APPROACH

by

SARAH ANN RAJALA

A THESIS SUBMITTED
IN PARTIAL FULFILLMENT OF THE
REQUIREMENTS FOR THE DEGREE OF

DOCTOR OF PHILOSOPHY

APPROVED, THESIS COMMITTEE:

Dr. R.J.P. de Figueiredo
Chairman

Dr. C.S. Burrus

Dr. L.D. Lutes

Houston, Texas

June, 1979

ABSTRACT

ADAPTIVE NONLINEAR IMAGE RESTORATION BY A

MODIFIED KALMAN FILTERING APPROACH

Sarah Ann Rajala

An adaptive nonlinear Kalman-type filter is presented
in this dissertation for the restoration of two-dimensional
images degraded by general image formation system
degradations and additive white noise. A vector difference
equation model is used to model the degradation process.
The object plane distribution function is partitioned into
disjoint regions based on the amount of spatial activity in
the image, and difference equation models are used to
characterize the object plane distribution function.

It is shown that each of the regions can be uniquely
characterized by their second order statistics. The
autocorrelation function for each region is then used to
determine the coefficients of the difference equation model
for each region. Recursive estimation techniques are
applied to a composite difference equation model.

If the images are to be restored for human viewing it
is desirable to account for the response of the human visual
system as part of the receiver characteristics. This is
done by weighting the variance σ^2 of the additive noise by a

visibility function, where the visibility function is a subjective measure of the visibility of additive noise in an image by the human visual system. As a consequence, the resulting effective variance depends nonlinearly on the state.

Two additional features are added to the new restoration filter to solve problems arising in the implementation phase. A nearest neighbor algorithm is proposed for the selection of a previously processed pixel for providing the previous state vector for the state of pixel (i, j). Secondly, a two-dimensional interpolation scheme is proposed to improve the estimates of the initial states for each region.

ACKNOWLEDGEMENTS

I extend my gratitude to my principal adviser Dr. Rui J. P. de Figueiredo for all the assistance he has given me throughout the period I worked on my dissertation. I also thank the members of my committee, Dr. C. S. Burrus and Dr. L. D. Lutes for their assistance in this effort.

A special thanks goes to my friends and my husband Jim Aanstoos for their patience, encouragement and love.

TABLE OF CONTENTS

CHAPTER 1

INTRODUCTION

I. Preliminary Remarks

Image restoration, image enhancement, pictorial pattern recognition, and encoding of images for storage or transmission are some of the areas included in the field of image processing. Each of these areas is concerned with different aspects and properties of an image, although a number of the same general techniques are utilized by more than one of these areas. A new technique is developed in this dissertation which lends itself primarily to the areas of restoration and enhancement. It is concerned with the improvement of image quality.

It is well known that no imaging system gives images of perfect quality, and it is because of this problem that the areas of restoration and enhancement have developed. There is a need to improve the quality of the images that are received from these systems.

The model generally used to represent a digital image formation system (Hunt [22]) appears in figure 1.1. The system response is,

$$g(i, j) = s\{h(i, j) * f(i, j)\} + \varepsilon_2 n_2(i, j) + n_3(i, j), \qquad (1-1)$$
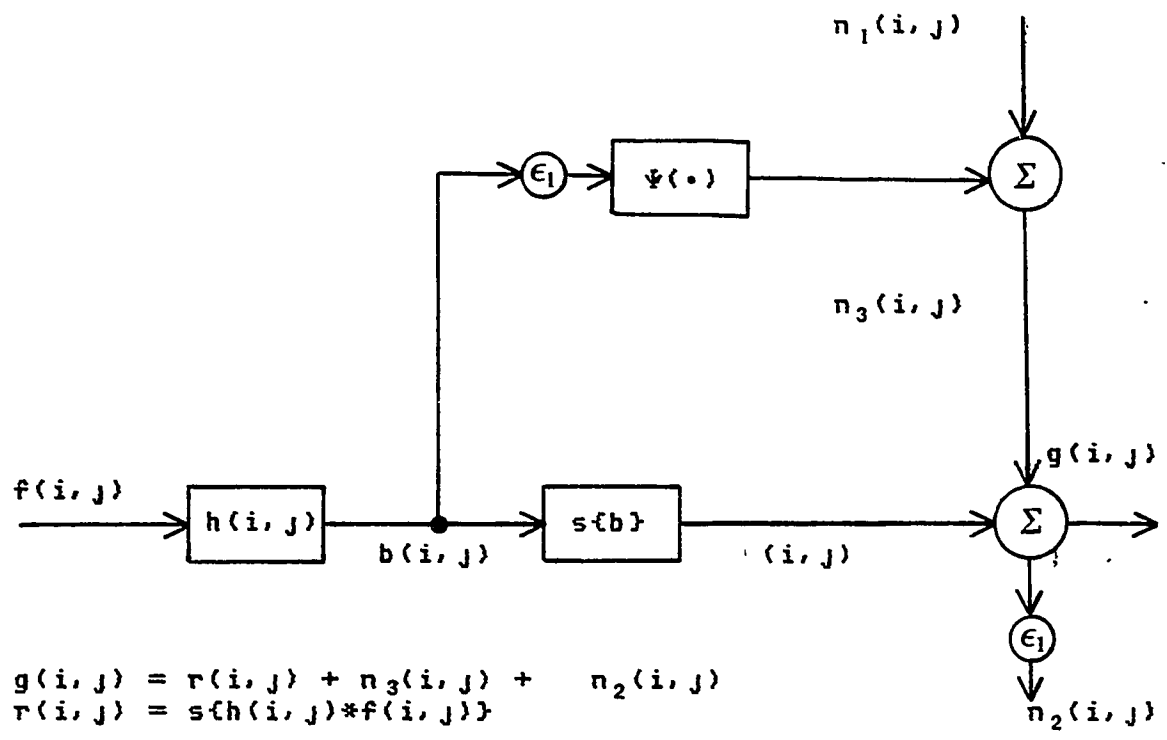
$g(i,j) = r(i,j) + n_3(i,j) + n_2(i,j)$
$r(i,j) = s\{h(i,j)*f(i,j)\}$

$f(i,j)$ — Object plane radiant energy distribution
$h(i,j)$ — Image formation system
$b(i,j)$ — Image plane radiant energy distribution
$s\{\cdot\}$ — Detector response (generally nonlinear)
$r(i,j)$ — Response variable of the detector
ϵ_1, ϵ_2 — Gain parameters
$\Psi(\cdot)$ — Feed forward function to account for
          signal dependent noise
n_1, n_2 — Noise processes
n_3 — Signal dependent noise
$g(i,j)$ — Response of the entire system

Figure 1.1

for $i = 0, 1, ..., M-1$ and $j = 0, 1, ..., N-1$, the extent of the two-dimensional image. Here, $g(i, j)$ is the recorded image distribution, $s\{\cdot\}$ is the detector response function, $h(\cdot, \cdot)$ is the image formation system response, $f(\cdot, \cdot)$ is the object plane radiant energy distribution, and the symbol $*$ represents the operation of convolution. The remaining two functions, $n_2(\cdot, \cdot)$ and $n_3(\cdot, \cdot)$ are noise processes; $n_2(\cdot, \cdot)$ is noise generated independently of the signal scaled by the gain parameter ε_2, and $n_3(\cdot, \cdot)$ represents signal dependent noise.

In the general case, the image formation system h can represent any number of possible distortions. As indicated by its name, the original intention was for h to represent the distortion caused in imaging systems, i.e. photographic equipment. It has since been generalized to include any distortion that is modeled by a linear system. This may include distortions from coordinate transformations, linear motion blur, or air turbulence.

The image formation system in figure 1.1 can be simplified in many situations. In general, it is assumed that the recording system response, $s\{\cdot\}$, can be approximated by a linear function. Actually this is true only for low contrast images. In any event, most of the restoration and enhancement techniques have been developed under the assumption that $s\{\cdot\}$ is linear and in fact $s=1$. If an image is of high contrast, the resulting nonlinearity can be accounted for by a zero-memory nonlinear filter.

Another simplification is that only signal independent noise is present in the system. In figure 1.1 we would only consider the noise source $n_2(i,j)$. In addition, if the system response is space invariant we can utilize certain properties from matrix theory for easier manipulation. For example, if the image formation system is linear space-invariant then [H] has block Toeplitz structure. We will represent [H] for this case by $[H_{BT}]$. Further reductions in the computational effort can then be made if $[H_{BT}]$ can be approximated by a circulant, when it is applicable. Once represented in terms of a circulant, the discrete Fourier transform can be utilized. On this aspect, much work has been done by Hunt [21], Ekstrom [8], and Gray [15].

In the area of image processing good reviews and bibliographies are provided by Huang, Schreiber and Tretiak [20]; Hunt [22]; Andrews and Hunt [4]; and Rosenfeld and Kak [48]. Several of the more pertinent techniques in both image enhancement and restoration will be reviewed in chapter 2 for understanding and comparison with the new technique proposed.

A considerable amount of work has been done on techniques in enhancement. The topic of geometrical distortions has been presented by Johnston and Rosenfeld [26]. Roetling [47] has worked on noise suppression, while Martelli and Montanari [34] have considered the problem of optimal smoothing, with application to fingerprints. Troy, Deutsch and Rosenfeld [57] have performed gray-scale

manipulations for texture analysis.

One of the basic approaches to image restoration has been the application of Wiener filtering with work done by Helstrom [18] and Slepian [53]. Sometime later, an extension of this basic approach was made to what is known as constrained least squares filtering. This has proved to be a flexible approach to image restoration. A considerable effort has been applied to this problem. It was first formulated by Phillips [42] and refined by Twomey [58], [59] in the one dimensional case. The actual implementation in two dimensions was accomplished by MacAdam [33] and by Hunt [21]. Another similar technique of interest is homomorphic image restoration. Oppenheim, Schafer and Stockham [41] did some of the original work on one-dimensional signals. Later, Cole [7] and Cannon [6] applied homomorphic filtering to images.

More recently, recursive estimation techniques have been applied to the area of image restoration in hopes of obtaining a better image restoration technique. Research has been done by Nahi and Assefi [37], Nahi and Franco [38], Aboutalib et al. [1], Woods [60], and Jain [25]. These techniques show promise in the development of an optimal image restoration filter.

II. Summary of the Results

This dissertation describes the use of the fundamental

theory of recursive least squares estimation as the basis for the development of an adaptive nonlinear Kalman-type filter for restoration of two-dimensional signals. A number of the currently existing problems are solved in an attempt to design a more nearly optimal restoration scheme. It is shown that recursive estimation provides a flexible approach to the problem of image restoration and admits a more accurate method for the description of the image model.

In an attempt to find this better restoration procedure it is necessary to consider any problems that currently exist and attempt to solve these in a manner that leads to the desired result. One of the fundamental problems with the existing image model used for the implementation of recursive estimation in two dimensions is that the object plane distribution is considered to be a single wide-sense stationary Markov process. This often leads to unsatisfactory restoration results. It is shown that a more accurate description of the characteristics of the object plane, i.e. the original undistorted object, is required. The model of the object plane distribution function is generalized to the case where it is considerd to be a wide-sense stationary process on each of a set of disjoint regions of the object distribution.

Another problem, originally pointed out by Netravali and Prasada [39] is the lack of use of receiver characteristics in the development of most restoration schemes. Specifically, in the case in which images are to

be utilized by human viewers the restoration scheme is improved by taking advantage of the characteristics of the human visual system. A method is devised to utilize such receiver characteristics in the design of a restoration filter for the system described by,

$$g(i, j) = h(i, j)*f(i, j) + n(i, j). \qquad (1-2)$$

This is accomplished by weighting the contribution of the additive noise by a visibility function. This visibility function is based on the ability of the human visual system to perceive random noise in an image. It is assumed that f is generated by a linear system b which has as its input a white noise source. The system impulse response b is determined such that the statistics of f are generated at the output.

A difference equation model is used to describe the image formation system represented by equation (1-2). This model is designed to realize the distortion point spread function h and account for the statistical nature of the object distribution function f in each of the regions. The additive noise is assumed to be Gaussian with zero mean and a known variance. The resulting set of difference equations for the kth region is:

$$\underline{x}_k(i, j+1) = A_k \underline{x}_k(i, j) + B_k \underline{u}_k(i, j), \qquad (1-3)$$

$$g(i, j) = \underline{c}_k^T \underline{x}_k(i, j) + n(i, j), \qquad (1-4)$$

where the noise process $n(\cdot)$ is such that $E[n(i, j)] = 0$ and $E[n(i_1, j_1)n(i_2, j_2)] = \sigma^2 \Delta(i_1 - i_2)\Delta(j_1 - j_2)$. The superscript T is used to denote the transpose of a matrix, and Δ represents the Kronecker delta function. The dimension of the state vector $\underline{x}$ is specified by the minimum order of the system distortion h and the system b. The input noise source vector $\underline{u}_k(i, j)$ generates $f_k(i, j)$, and is such that $E[\underline{u}_k(i, j)] = 0$ and $E[\underline{u}_k(i_1, j_1)\underline{u}_k(i_2, j_2)^T] = R_k \Delta(i_1 - i_2)\Delta(j_1 - j_2)$. The restoration filter that results from this model is realized in a recursive fashion.

In addition to the theoretical formulation of this generalized adaptive nonlinear Kalman-type filtering scheme, a new implementation is proposed to further optimize the restoration procedure. If the amount of spatial activity in the image is great, the recursive estimation scheme may not be able to respond as quickly as the image changes in intensity level. In order to speed up the response of the filter in regions where the spatial activity is greater than the response of the filter, a reinterpretation of the definition of the previous state in two-dimensional recursive estimation schemes is given. It is proposed that the previous state of pixel (i, j) may not be best specified by pixel $(i, j-1)$. A nearest neighbor criterion is utilized

to determine which of the pixels in the neighborhood of the pixel is really the best previous state. These developments are presented in Chapter 3.

Chapter 4 is devoted to a description of the algorithm developed and of the implementation procedure used in testing this restoration method, with a presentation of the results. Finally, Chapter 5 will present the conclusions of this development and comparisons with existing techniques.

CHAPTER 2

HISTORICAL REVIEW

I. Introduction

This chapter presents a review of the presently available techniques in image enhancement and restoration. The emphasis in this discussion is on those techniques which are directly applicable to the development of the research developed in this dissertation. Section II describes the general background knowledge in image enhancement. Much of this material has led to a more complete understanding of the image restoration problem. The third section is on the techniques of image restoration. Many of the fundamental techniques will be reviewed briefly for general information and comparison. The techniques which are fundamental to this thesis will be developed in detail.

Prior to discussing the details of the enhancement and restoration techniques, it is necessary to understand the difference between these two approaches to image processing. Image restoration improves the quality of an image by compensating for the effects of a specific known or estimated degradation process. Image enhancement improves image quality without actual knowledge of the degradation process involved. Its objective is to improve the quality of the image with respect to a predetermined standard.

II.   Image Enhancement

Initially, a standard must be established for measuring the quality of the image being processed.   The quality of an image is a somewhat subjective measure of the accuracy to which certain defined information in the image is measured. The definition of quality in a given set of images is dependent on the purpose for which they are intended. A picture may be needed for precise measurements or it may be used for casual human viewing.   The degree and type of degradations that would be objectionable in one case may not be in the other. Two standards commonly used for measuring objective image quality are resolution and acutance.

Resolution of an image describes the accuracy with which one can distinguish small, close objects in the image. Acutance is a measure indicating the average steepness of an edge in the output image that results from a perfect step in the input image. Both resolution and acutance are commonly utilized in determining the degree to which the enhancement operations are successful. More details of these and other measures of image quality can be found in a paper by Levi [30].

There are many different operations used to enhance the quality of an image. Four of the most common operations will be discussed briefly. The first operation is gray scale modification, (Troy, Deutsch, and Rosenfeld [57]). There are two approaches used for the modification of the gray

scale of an image. One is gray scale correction and it is used to modify gray levels of the individual picture points or pixels, to compensate for uneven exposure when the picture was originally recorded.

The second 0 approach to modification is gray scale transformation. This method changes the gray scale in a uniform way throughout the picture, usually to increase the contrast. The method is performed by mapping from the given gray scale z to a transformed gray scale z',

$$z' = t(z). \qquad (2-1)$$

An important special case of gray scale transformation is histogram modification which assigns a specified distribution of gray levels to a picture. One example where histogram modification is used is quantization of a picture into K discrete levels in such a way as to minimize quantization error. The K levels should be spaced close together in heavily populated regions and further apart in sparse regions.

Operation two is known as geometric correction. Johnston and Rosenfeld [26]; Sawchuk [50]; and O'Handley and Green [40]. have considered various types of distortion including perspective distortion, the result of taking a picture from an oblique viewing angle, and pincushion or barrel distortion, the distortion due to limitations of optical imaging or electronic scanning.

An arbitrary geometric distortion can be defined by equations that relate the undistorted coordinate system (x, y) to the distorted coordinate system (x', y'). In the general form they are,

$$x' = b_1(x, y) \quad \text{and} \quad y' = b_2(x, y). \quad (2-2)$$

The third type of operation for the enhancement of images is sharpening, and Stockham [54] and O'Handley and Green [40] have worked on this method. Blurring is generally caused by an averaging or integrating operation, so one might expect that sharpening could be done by differential operations. Several methods have been developed to compensate for the problem of blurring. These include the use of the gradient, the Laplacian, and high emphasis filtering, all of which compensate for the effects of averaging by differentiating and/or emphasizing the high spatial frequency content (Goldmark and Hollywood [13] and Kovasznay and Joseph [29]).

Finally, the operation of smoothing is utilized for the removal of unwanted noise (Martelli and Montanari [34]). Of course, one must be careful with smoothing not to blur the image. A general approach to smoothing is to define a cost function $\emptyset$ for evaluating the various possible smoothings f of a given noisy picture g. The cost function $\emptyset$ depends on both the irregularities of f and the discrepancy between f and g. Noise removal can be taken care of in several

different ways, and the method is generally dependent on the type of noise present.

III.   Image Restoration

The objective in image restoration is to compensate for a known or estimated distortion causing an image to be degraded. That is, an attempt is made to determine the original object distribution f given the recorded image g and the point spread function (PSF) h. This entails designing a filter to invert the distortion. There have been two general categories of techniques used in designing image restoration filters. One category is based entirely on the knowledge of the distortion and assumptions about the image formation system. No attention is given to the resolution of the image. The second category is based on the fact that the image will be used for human viewing and resolution of the image should be considered. There are many methods available for restoration of the type discussed in category one. However, in category two, only one approach has been reported for the restoration of images, although these same ideas have been utilized to a great extent for image coding problems.

In the first category of restoration methods there are two basic subgroups of techniques. One is that of noniterative restoration techniques and the other that of linear algebraic techniques. The noniterative restoration

techniques are governed by the following assumptions: (1) There exists only signal independent noise. (2) A linear approximation can be made for the nonlinear detector s. This is known as a low contrast assumption, and in fact without loss of generality it can be assumed that s=1. (3) It is assumed that the systems are space-invariant and therefore Fourier techniques can be applied. (4) It is assumed that when a segment is cut away from a larger image the restoration effects can be localized, i.e. the border effects can be neglected.

There are three specific methods in this category which will be discussed: least squares filtering, minimum-mean-square-error filtering, and homomorphic filtering. The general model is

$$g = [H_{BT}]f + n, \qquad (2-3)$$

where g, f, and n are lexicographically ordered vectors, and [H] is the matrix resulting from the point spread function. Invoking least-squares restoration is equivalent to minimizing the norm of the noise term n. The rationale behind this is that, in the absence of any specific knowledge about n, a solution is sought which is consistent with having n as small as possible. The resulting least squares estimate is,

$$f = [H_{BT}]^{-1} g. \qquad (2-4)$$

There are two immediate problems with this technique. One is the ill-conditioned nature of the PSF matrix. We may not be able to invert $[H_{BT}]$. The second problem, also a result of this ill-conditionedness, is that inverting $[H_{BT}]$ can really amplify the noise term; yet if $[H_{BT}]$ is not ill-conditioned this is one of the most straightforward methods for restoring an image.

In minimum mean square error (MMSE) filtering a solution is found to minimize the difference between the original object distribution f and the restored object distribution $\hat{f}$. Let the total error of estimation, ε, be defined by

$$\varepsilon = f - \hat{f}. \qquad (2-5)$$

The MMSE criterion requires the total error of estimation to be a minimum over the entire ensemble of all the possible images. Since this error, ε, could be a positive or negative quantity, consider the positive quantity $\varepsilon^T\varepsilon$. The criterion then is to minimize the expected value of $\varepsilon^T\varepsilon$. Assuming that a linear estimate exists, i.e. $\hat{f} = [L]g$, the following MMSE restoration filter results:

$$[L] = [R_f][H_{BT}]^T([H_{BT}][R_f][H_{BT}]^T + [R_n])^{-1} . \qquad (2-6)$$

One drawback occurs in the low signal to noise ratio (SNR) cases, when the result is not good. Several reasons

are possible for the inadequacy of this filter at low SNR. The MMSE estimate is based on linear assumptions, even though nonlinearities exist in the recording and human visual systems. Secondly, MMSE is not the criterion the human visual system uses for low noise situations; MMSE appears much too smooth. Finally, MMSE assumes a stationary model, which is not sufficient to model the degradation.

Homomorphic filtering was originally proposed by Stockham, Oppenheim, and Schafer [41] in the area of digital signal processing. It was later extented to two-dimensional applications by Cannon [6]. This technique maps the image signal from the original space to another space with desirable properties for easier manipulation. The assumptions and model remain the same for this approach. The criterion, however is different. Power spectrum equalization is utilized here. This means a linear operator [L] must be found, such that when this [L] operates on g, the result is an image f with a power spectrum equal to the power spectrum of f. This leads to an inverse filter described by,

$$|L(u,v)| = \left[\frac{P_f(u,v)}{P_i(u,v)} \right]^{1/2} . \qquad (2-7)$$

It should be noted that this technique specifies only the magnitude of the filter. It is generally assumed that the phase is either zero or previously given.

All three of these filters work reasonably well when

there is a high SNR. In fact, they all converge to the least squares filter. The advantage of one method over the other in this situation will depend on the amount of a priori information. Homomorphic filtering can construct the information needed for restoration from the degraded image itself, by estimating ϕ_f and ϕ_n. MMSE requires the most a priori information, while the least squares approach is somewhere in between.

With respect to visual quality, homomorphic filtering produces the best results for medium to low SNR. Least squares and MMSE are both much worse. All these techniques are fairly straightforward and the number of computations are considerably reduced when Fourier techniques can be applied. However, this greatly restricts the class of images to which these techniques can be applied. What happens if the distorting process is not space-invariant? This question leads us to the second group of restoration techniques in this category, the one that considers the human visual characteristics.

The algebraic techniques allow one to use a more general class of images to be processed. The assumptions for this category of images are: (1) only signal independent additive noise will be considered. (2) The detector response will again be assumed to be linear. (3) However, in this case it will be assumed that the distorting process can be spatially-variant. All filters developed in this section will be derived by a least-squares Lagrangian

approach.

The image formation model is now,

$$g = [H]f + n. \qquad (2-8)$$

An objective function, $W(f)$ is defined as the function which specifies the criterion for the restoration technique being developed.

The inverse filter requires the minimization the norm of the difference between the image and the reblurred object. The objective function becomes,

$$W(f) = \|g - [H]f\|^2. \qquad (2-9)$$

Solving for the estimate $\hat{f}$ yields,

$$\hat{f} = ([H]^{*T}[H])^{-1} [H]^{*T}g, \qquad (2-10)$$

where the superscript * denotes the complex conjugate. It is assumed that [H] is not singular. In the case of a spatially invariant image formation system [H] this is the least squares case of the last section. It has the same problems as the least squares filter in either case.

Since it is often the case that [H] may be singular, one would like to design a filter which has more control over the restoration process, i.e., one which places some constraint on the design procedure. If we have some a priori

knowledge about f, for instance we might know that f is a smooth function, then an additional constraint could be added to minimize a roughness measure, such as the norm of the second derivative (or in the case of discrete images, the second difference). In general we minimize the norm of a linear operation on f, $[Q]f$, subject to the usual conditions on the noise. If the norm of the noise is known or measurable, then we minimize $\|[Q]f\|^2$ subject to $\|g - [H]f\|^2 = \|n\|^2$. In this case, the objective function is

$$W(f) = \|[Q]f\|^2 - \lambda(\|g - [H]f\|^2 - \|n\|^2). \qquad (2-11)$$

The constrained least squares estimate (Hunt [21]) is

$$\hat{f} = ([H]^{*T}[H] + \gamma[Q]^{*T}[Q])^{-1}[H]^{*T}g, \qquad (2-12)$$

where $\gamma = 1/\lambda$.

The constrained least squares restoration is a fairly general approach to restoration. This results from the general nature of the function $[Q]$, which can represent a number of possible constraints. Some of these include, $[Q] = [I]$ which leads to the pseudo-inverse filter; $[Q] =$ finite difference matrix which, as discussed above gives the constrained least squares filter, $[Q] =$ eye model, which leads to restoration from a visual perception point of view, and $[Q] = [\phi_f]^{-1/2}[\phi_n]^{1/2}$ yielding the parametric Wiener filter.

One other type of filter is the maximum entropy filter (Frieden [12]), which is based on modeling the object as a probability density function. If f is normalized to unit energy, then each f can be treated as a probability. One reason this approach is so appealing is that it guarantees positive values in the restored image.

The objective function for the derivation of the maximum entropy filter is

$$W(f) = f^T \ln f - \lambda \{ \|g - [H]f\|^2 - \|n\|^2 \}. \qquad (2-13)$$

After taking the partial derivative and setting it equal to zero we obtain,

$$\ln \hat{f} = -\underline{1} - 2\lambda [H]^{*T}(g - [H]f). \qquad (2-14)$$

It should be noted that this is a nonlinear solution. This problem is in general very difficult to solve. One approach to solving equation (2-14) is to linearize it. This simplifies the solution, but it also reduces the effectiveness of the filter.

The following restoration technique is based on the application of recursive estimation to the problem of image restoration (Aboutalib, et al. [1]). A number of people have done work in this area with promising results, and it is on this theoretical development that the restoration filter proposed in this thesis is based. The development of

this method will be explained in considerable detail. Again, it is assumed that the recorded image is defined by the brightness function g, and the object plane brightness function is f. In the case where the point spread function is assumed to be space invariant, we can represent g by the following equation:

$$g(i,j) = \sum_{q=-\delta}^{\theta} \sum_{m=-\gamma_q}^{\Gamma_q} h(q,m)f(i-q, j-m) + n(i,j). \qquad (2-15)$$

The noise is again assumed to be additive, white, Gaussian noise. $\delta, \theta \geq 0$ is the vertical extent of the blur, h is the point spread function, and $\gamma_q, \Gamma_q \geq 0$ is the horizontal extent of the blur along horizontal line i-q. It is assumed that $h(k, -\gamma_q) = 0$ for $\delta \leq q \leq \theta$. Let us make the following transformation of variables to ease the ensuing development. Let $\phi_q = \gamma_q + \Gamma_q$ and use the notation $r_{qm} = h(q, m-\gamma_q)$. Equation (2-15) becomes

$$g(i,j) = \sum_{q=\delta}^{\theta} \sum_{m=0}^{\phi_q} r_{qm} f(i-q, j-\gamma_q-m) + n(i,j). \qquad (2-16)$$

The image intensity can be written in terms of the horizontal shift operator, $D^p f(i,j) = f(i, j-p)$. The contribution to g(i,j) from the object line i-q is,

$$g_q(i, j) = [r_{q0} + r_{q1} D +, \ldots, + r_{q\phi_q} D^{\phi_q}]$$

$$f(i-q, j+\Gamma_q) + n(i, j). \tag{2-17}$$

Define a function of the delay operators, $H_q(D) = r_{q0} + r_{q1} D +, \ldots, + r_{q\phi_q} D^{\phi_q}$ for $\delta \leq q \leq \theta$. The total contribution from all the $\delta + \theta + 1$ object lines is then

$$g(i, j) = \sum_{q=-\delta}^{\theta} H_q(D) f(i-q, j+\Gamma_q) + n(i, j). \tag{2-18}$$

If $L = \max\{\Gamma_q : -\delta \leq q \leq \theta\}$ is the maximum degree of anticipation of the blur over all contributing lines and

$$\underline{f}(i, j) = col[f(i-\theta, j), f(i-\theta+1, j), \ldots, f(i+\theta, j] . \tag{2-19}$$

We can write the vector of causal moving average operator polynomials as,

$$\underline{H}(D) = col[H_\theta(D) H_{\theta-1}(D) \ldots H_{-\delta}(D] , \tag{2-20}$$

and the delay matrix as

$$M(D) = diag(D^{L-\Gamma_\theta}, D^{L-\Gamma_{\theta-1}}, \ldots, D^{L-\Gamma_{-\delta}}). \tag{2-21}$$

The system equation now becomes,

$$g(i, j) = \underline{H}^T(D) M(D) \underline{f}(i, j+L) + n(i, j), \tag{2-22}$$

for $i, j = 0, 1, \ldots, N-1$.

Note that the problem is formulated such that the blur is multi-input. In addition, $\underline{f}(i, j+L) = D \ \underline{f}(i, j)^{-L}$ is composed of object intensities from each of the $\delta+\Delta+1$ lines contributing to line i. Thus, $\underline{f}(i, j+1)$ is a vector that scans the object plane. Now, define

$$\underline{s}(i, j) = M(D)\underline{f}(i, j+L). \qquad (2-23)$$

The system description is

$$g(i, j) = \underline{H}^T(D)\underline{s}(i, j) + n(i, j), \qquad (2-24)$$

where $\underline{s}(i, j)$ is the input vector, $\underline{H}^T(D)$ is a multi-input-single-output causal operator. Under this formulation, the system admits a recursive realization as follows:

$$\underline{x}(i, j+1) = \widetilde{A}\underline{x}(i, j) + \widetilde{B}\underline{s}(i, j), \qquad (2-25)$$
$$g(i, j) = \widetilde{\underline{c}}^T\underline{x}(i, j) + \widetilde{\underline{d}}^T\underline{s}(i, j) + n(i, j), \qquad (2-26)$$

for $i, j = 0, 1, +\ldots, -1$, where $n(i, j)$ is white with $E[n] = 0$ and $E[n^2] = \sigma^2$.

Under the assumption that the object plane may be modeled as a zero-mean, two-dimensional stationary random field, with a known correlation function, a difference equation model can be developed which, when driven by white noise, produces an output whose statistics match the

statistics of $\underline{s}(i,j)$. This is represented by

$$z(i,j+1) = P\underline{z}(i,j) + Q\underline{u}(i,j), \qquad (2-27)$$

$$\underline{s}(i,j) = T\underline{z}(i,j), \qquad (2-28)$$

where $E[\underline{u}] = 0$ and $E[\underline{u}\underline{u}^T] = R$.

The degradation model can now be augmented with the object model to yield the following composite model:

$$\underline{w}(i,j+1) = A\underline{w}(i,j) + B\underline{u}(i,j), \qquad (2-29)$$

$$g(i,j) = \underline{c}^T\underline{w}(i,j) + n(i,j), \qquad (2-30)$$

where $\underline{w}^T(i,j) = [\underline{x}^T(i,j)\underline{z}^T(i,j)]$, and

$$A = \begin{bmatrix} \widetilde{A} & \widetilde{B}T \\ 0 & P \end{bmatrix} \quad B = \begin{bmatrix} 0 \\ Q \end{bmatrix} \quad \underline{c}^T = [\underline{\widetilde{c}}^T \ \underline{\widetilde{d}}^T T].$$

The best linear minimum variance estimate $\underline{\hat{w}}(i,j|j)$ of $\underline{w}(i,j)$ can now be developed based on the observations $\{g(i,t), t=0,\ldots,j\}$. The following Kalman filtering equations result,

$$\underline{\hat{w}}(i,j|j) = [I - \underline{\Phi}(j)\underline{c}^T]A\underline{\hat{w}}(i,j-1|j-1) + \underline{\Phi}(j)g(i,j), \qquad (2-31)$$

$$\underline{\Phi}(j) = P(j)\underline{c}[\underline{c}^TP(j)\underline{c} + \sigma^2]^{-1}, \qquad (2-32)$$

$$P(j+1) = A[I - \underline{\Phi}(j)\underline{c}^T]P(j)A^T + BRB^T, \qquad (2-33)$$

for i, j = 0, 1, ..., N-1, and with $\underline{w}(0) = \underline{w}_0$, $P(0) = P_0$. $P(j)$ is defined as the estimation error covarince matrix and $\underline{\Phi}(j)$ is the Kalman gain vector. The best linear minimum variance extimate of $\underline{s}(i, j)$ based on the observations $g(i, t)$ for t=0, 1, ..., j is

$$\underline{s}(i, j) = [O \ T]\hat{\underline{w}}(j|j). \quad (2\text{-}34)$$

$\underline{s}(i, j) = M(D)\underline{f}(i, j+L)$, as before.

This method is a good way to restore images which are of relatively low contrast. Unfortunately, when there is a lot of spatial activity in the image the filter cannot keep up with the changes in the image. The result is then an undesired smoothing of the edges. The advantages of this method, though, are that it is quite easily implemented via a digital computer and there is the ability to model the object plane statistics.

The second category of image restoration techniques is based on a subjective criterion. The initial work has been done by Anderson and Netravali [2]. The basis for this approach is that the restored images will be for human viewing, so one would like to utilize those properties of the human visual system (HVS) which are engaged in discerning information and removing noise from an image. The assumptions for this restoration procedure are: (1) the recorded image is simply the sum of the original object and white Gaussian noise, specifically,

$$g(i,j) = f(i,j) + n(i,j); \qquad (2-35)$$

and (2) n is a zero-mean, white, Gaussian noise source independent of f and of unknown but constant variance v_n.

To develop the procedure first construct a measure of the spatial detail in an image (Netravali and Prasada [39]). It is known that at sharp transitions in image intensity the contrast sensitivity of the HVS decreases with the sharpness of the transition and increases exponentially (within limits) as a function of spatial distance from the transition. This information is used to define the following measure of spatial detail, called the masking function:

$$M_{kr}(i,j) = \sum_{p=i-k}^{i+k} \sum_{q=j-r}^{j+r} C^{\|(i,j)-(p,q)\|} [|m_{ij}^v| + |m_{ij}^h|], \qquad (2-36)$$

where $\|(i,j)-(p,q)\|$ denotes the Euclidean distance between points (i,j) and (p,q); m_{ij}^v and m_{ij}^h are the vertical and horizontal slopes of the image intensity at (p,q), respectively; C is a constant controlling the rate of exponential decay of the effect of a transition of image intensity on its neighbors; and k and r are constants controlling the size of the relevant neighborhood around (i,j).

The second step in this procedure is to determine the relationship between the visibility of noise in an image and the masking function. This relationship is known as the

visibility function and gives the relative visibility of a unit noise added to all points in a picture where the measure of spatial detail, M_{kr}, has a certain value. The visibility function is determined by a number of subjective tests. Test images are computed and stored. The masking function M_{kr} is computed for each pixel of the original image. A masking value γ and a noise power V_n are chosen. To each pixel of the original image whose masking value M_{kr} is in the range $[\gamma - \Delta\gamma/2, \gamma + \Delta\gamma/2]$, where $\Delta\gamma$ is a small increment, white Gaussian noise of power V_n is added. The test image so obtained is characterized by the values γ and V_n . For each γ at which we wish to measure the visibility $f(\gamma)$, three test images with noise powers $V_{n_1}, V_{n_2}, V_{n_3}$ are generated.

A subjective test is performed under which the experimenter randomly selects a test image to which he adds just enough white noise to reach a point of subjective equivalence between the two pictures. If V_{w_1}, V_{w_2}, and V_{w_3} are the equivalent white noise powers selected by the subject corresponding to test images which have $V_{n_1}, V_{n_2}, V_{n_3}$ amounts of noise, then, assuming proportionality, the visibility function is defined as

$$V(\gamma) = \frac{1}{\Delta\gamma} \frac{V_{w_1} + V_{w_2} + V_{w_3}}{V_{n_1} + V_{n_2} + V_{n_3}} , \qquad (2\text{-}37)$$

where γ is the masking value and V_n is the noise power. The visibility function decreases with respect to its argument

because at higher masking function values we add noise to fewer picture elements and the perception of noise at picture points having higher masking value is decreased. The visibility function is used to determine the coefficients of the restoration filters. Two types of filters were developed, the S-type filter and the SD-type filter.

The S-type filter computes a local average of (2q+1) neighboring elements,

$$\hat{s}_k = \sum_{i=-q}^{q} a_i^{\ k} \ z_{i+k} \ . \qquad (2\text{-}38)$$

This filter was chosen because the $a_i^{\ k}$ can be changed for each $\hat{s}_k$ according to the visibility function. The a's are subject to the usual constraints on filter coefficients, i.e., a ≥ 0, for i = -q,...,q and $\underline{a}^T\underline{u} = 1$.

The variance of the noise in the image g(i,j) is v_n , assumed constant over the entire image. The amount of noise remaining after the filter is applied is var {s} = $v_n\underline{a}^T\underline{a}$. We can define $v_a = \underline{a}^T\underline{a}$ as the relative amount of noise passed by the filter. As we have noted previously, the application of an averaging filter to an image results in some blurring. Since it is important that this blurring be kept to a minimum, a measure of this blurring is defined and is called the spread,

$$w_a = \sum_{i=-q}^{q} a_i^{\ 2} \ i^2 = \underline{a}^T\underline{S}\underline{a}, \qquad (2\text{-}39)$$

where $\underline{S}$ is the spread matrix.

The requirements for the filter weights $\underline{a}$ are that they have good noise suppressing power but a small tendency to blur. These are opposing goals. Consequently, the objective function is defined as follows:

$$J(\underline{a}) = \alpha v_a + (1 - \alpha)w_a = \underline{a}^T[\alpha\underline{I} + (1 - \alpha)\underline{S}]\underline{a}, \qquad (2-40)$$

subject to $\underline{u}^T\underline{a} = 1$. Using Lagrangian methods we obtain the solution,

$$\underline{a} = \lambda[\alpha\underline{I} + (1 - \alpha)\underline{S}]^{-1} \underline{u}, \qquad (2-41)$$

where λ is adjusted to ensure that $\underline{u}^T\underline{a} = 1$. α is a tuning parameter whose value varies from 0 to 1. As α changes the filter changes from a sharply peaked filter to a flat, equally weighted averaging filter.

Thus far, in the description above, a tunable filter to be applied to a neighborhood of a given pixel has been constructed. The visibility function is now used to tune the filter via the parameter α. It is assumed that the visibility function has been scaled so that $f(0) = 1$. Let Q be the number of elements in the two-dimensional filter, and then choose a number ϕ, $(1/Q) \leq \phi \leq 1$, a constant for a given image, which determines the amount of noise passed by the filter in a perfectly flat area of the image. That is, set α so that

$$v_a = \emptyset \qquad\qquad (2\text{-}42)$$

at a pixel where $M = 0$ and $f(M) = 1$. In areas that are not flat choose α such that

$$v_a f(M) = \emptyset. \qquad\qquad (2\text{-}43)$$

This rule is applied at every pixel and results in uniform subjective noise visibility. If v_a is permitted to rise in busy areas, the spread goes down, producing a sharper filter. To allow for this variability, we introduce another tuning factor γ to control the way in which the filter responds to the visibility function. Equation (2-43) now becomes

$$v_a f^{\gamma}(M) = \emptyset. \qquad\qquad (2\text{-}44)$$

This restoration method is based on a measure of spatial detail that corresponds to that of the human visual system. In addition, two numbers, $\emptyset$ and γ, were chosen to give control of the overall amount of filtering and to regulate the degree of adaptivity, respectively. It would be desirable if in addition this procedure could recognize when the filter overlaps a prominent edge and would automatically reduce the overlapping filter weights. This would reduce the distorting influence of a nearby edge and hence preserve edge sharpness. This leads us to the second

type of filter, the SD-type filter.

The SD-type filter is a distortion-penalizing filter, so it is necessary to define a measure of distortion,

$$d_a = \sum_{i=-q}^{q} (z_{i+k} - z_k)^2 a_i^2 = \underline{a}^T \underline{D}\underline{a},\qquad (2\text{-}45)$$

where $\underline{D}$ is the distortion matrix. The objective function for this method is,

$$J(\underline{a}) = \alpha v_a + (1 - \alpha)(w_a + \theta d_a)$$

$$= \underline{a}^T[\alpha \underline{I} + (1 - \alpha)(\underline{S} + \theta\underline{D})]\underline{a},\qquad (2\text{-}46)$$

subject to $\underline{a}^T \underline{u} = 1$, and using θ as a tuning parameter.

It is readily seen that $\underline{D}$ represents a penalty applied to $\underline{a}$. When $\underline{a}$ overlaps an edge, there is a large difference between the brightness at the center of the filter and the brightness at a point across the edge. The penalty is then large forcing the coefficient a to be small.

In review, it should be noted that the main feature of these filters is that they are applied locally under the direction of a local fidelity criterion based on psychovisual principles. The S-type filter is tractable and convenient, but has a tendency to blur at prominent edges. This problem is accounted for in the SD-type filter and leads to better restoration. Unfortunately the price for this improvement is paid in an increased number of

computations.

In comparing the results of the restoration techniques in categories one and two, we must remember the fundamental differences in their original objectives. The category one techniques are based on the philosophy that images can be improved by designing a filter which inverts the distortion in the system. If there is noise in the response, the inversion is done subject to minimizing the norm of the noise. Category two techniques design the restoration filter, for removal of noise only, under the assumption that images will be used for human viewing. Therefore, the restoration filter is designed to choose the same desirable features in an image that the human visual system would choose.

There are important aims in the techniques of both of the catagories. Attempting to invert the distortion present in the system is a logical approach. In light of the fact that images are generally utilized by human viewers, taking into account certain aspects of the human visual system is desirable.

CHAPTER 3

AN ADAPTIVE NONLINEAR KALMAN-TYPE FILTER

I.   Introduction

      This chapter presents the theoretical development of an
adaptive nonlinear Kalman-type filter to be utilized for the
restoration of two-dimensional images.   This development
proceeds in a step by step fashion, solving several of the
problems inherent in the approaches currently used for the
restoration of images.

      One such problem is the necessity of using the receiver
characteristics in the design of the restoration filter for
the general model given in figure 1.1. Since the receiver
for many images is a human observer, it is desirable to
utilize the properties of the human visual system in
designing a better image restoration procedure.   In the
present work, the response of the human visual system to the
additive white noise present in an image is used in the
development of the adaptive nonlinear Kalman-type filter for
the system described by equation (1-1).

      Another problem results from the assumption that the
object   plane   distribution   function   f   is   usually
characterized by a single wide-sense stationary Markov
process. If there is a large spread in the amount of spatial
activity, this tends to yield an autocorrelation function

which has less resolution than is needed to characterize sharp edges. This problem is solved in the present work by partitioning the object plane into regions according to local spatial activity.

This partitioning also helps in reducing the large effort associated with the calculation of the restoration filter. Spectral factorization is necessary for the determination of the coefficients in the difference equations of the dynamic model used in the derivation of the restoration filter. The necessary operations are performed on much smaller matrices in the present approach.

Two problems are encountered in the implementation of the adaptive nonlinear Kalman-type filtering algorithm developed here. The first problem arises from the fact that the best choice for the previous state vector for the pixel (i,j) need not be the one associated with the pixel $(i,j-1)$. This is apparent at the boundary between two regions. Pixel $(i,j-1)$ may be in a region whose autocorrelation function differs widely from that of the region to which pixel (i,j) belongs; thus utilizing the state vector at $(i,j-1)$ as the one previous to the state vector at (i,j) may give poor results. This makes it necessary to determine a procedure for selecting among the previously processed pixels, one whose state should be used as the previous state vector. In the present work, this problem is solved by using a nearest neighbor criterion to determine the best selection of the previous state in the recursive restoration algorithm.

The second problem encountered is the lack of good initial condition information for the starting points in the regions. This problem is overcome by employing a two-dimensional interpolation (smoothing) scheme to obtain better estimates of the initial state vectors.

The solution of these problems has resulted in the development of the present adaptive nonlinear Kalman-type filtering scheme for the restoration of images. The four primary improvements offered by the filter are:

(1). The use of the visibility function to incorporate the properties of the human visual system as receiver characteristics; this is achieved by making the "effective" observation noise covariance depend nonlinearly on the state.

(2). The partitioning of the image into regions to allow for more accurate modeling of the second order statistics of the object plane distribution function according to spatial activity;

(3). The utilization of a nearest neighbor algorithm to determine the best previous state at boundaries and in regions of high spatial activity; and

(4). An interpolation scheme for the improvement of initial condition information.

In addition, our filter is capable of removing general image formation degradations by taking into account the

dynamics of the image formation system.

The following section establishes the validity of using the autocorrelation function as a property for describing the regions of the object plane. Next, a criterion function is presented which partitions the image into regions. In addition, a scheme is developed for the implementation of this partitioning process.

II. Image Partitioning adapted to Local Spatial Activity

Consider the problem of characterizing the object plane distribution function. In the previous literature (Aboutalib, et al. [1], Franks [9], Jain [25], Nahi and Assefi [37], Nahi and Franco [38], Woods and Radewan [60]), the object plane distribution function f has been represented by a wide-sense stationary process whose autocorrelation function is of the following form

$$R_f(\tau, \sigma) = K_1 \exp[-\alpha|\tau| - \beta|\sigma|], \qquad (3-1)$$

where τ and σ are horizontal and vertical displacements, respectively. This may not always be the case and can in fact lead to undesirable results. In particular, if there is large spread in the spatial activity content in the object plane, the constants K_1, α, and β may vary considerably from one area of the image to another, where spatial activity is defined as the rate of change of spatial

luminance from one pixel to another. This is directly related to the autocorrelation function through the parameters α and β. These two parameters specify the average number of statistically independent luminance levels in the horizontal, α, and the vertical, β, directions. Then, if the spatial activity is high, α and β will be greater than when the spatial activity is low. In what follows, an attempt is made to categorize the information in the object plane in such a way that regional autocorrelation functions can be used in lieu of one global autocorrelation.

It is necessary to guarantee that we have a meaningful set of features to be used to describe the information in the object plane. Several types of features may be considered. These include spectral, textural and contextural features. Spectral features describe the average tonal variations in the various bands of the spectrum. Textural features reveal the spatial distribution of tonal variations, and contextural features are those which yield information obtained from the regions surrounding an area being analyzed.

The problem at hand then is to find a property R_f such that an image can be partitioned into regions Ω_p for $p = 1,\ldots,k$. Each region Ω_p is to be restored utilizing this property R_f to yield an optimal restoration procedure.

One class of features particularily suited to recursive estimation techniques is that of spectral features. These are often represented in terms of the autocorrelation or

spectral density to yield information about the statistics of an image being restored.

Since the autocorrelation is dependent on the spatial activity of the area, it is reasonable to choose the regions Ω_p based on the amount of spatial activity in the image. There are a number of ways to partition f based on the amount of spatial activity. One is to utilize a bank of bandpass filters and separate the image strictly by the spatial frequency content at each pixel. Another approach is to use a function based on the amount of spatial activity as defined by the slope information at the pixel. This type of measure corresponds closely to the information represented by the autocorrelation function and will therefore be used. It has already been shown, in the preceding chapter, that the masking function is indeed a measure of the spatial activity in a neighborhood of a pixel.

Consider the masking function introduced in Chapter 2.

$$M_{kr}(i,j) = \sum_{p=i-k}^{i+k} \sum_{q=j-r}^{j+r} C^{\|(i,j)-(p,q)\|} [\,|m_{ij}^{v}| + |m_{ij}^{h}|\,], \quad (3-2)$$

where $\|(i,j) - (p,q)\|$ is the Euclidean distance between points (i,j) and (p,q); m_{ij}^{v} and m_{ij}^{h} are the vertical and horizontal slopes of the image intensity at (p,q); C is the constant controlling the rate of exponential decay; and k and r are the constants controlling the size of the relevant neighborhood around (i,j).

If the constants k and r are equal to zero, we have a measure of the spatial activity in the horizontal and vertical directions.

$$M_{00}(i, j) = |m_{ij}^v| + |m_{ij}^h|. \qquad (3-3)$$

It is desirable to extend this measure of spatial activity to include slope information in the immediate neighborhood of a given pixel. The immediate neighborhood of a pixel is assumed to include its eight nearest neighbors. Equation (3-3) is generalized to include information about the slopes in the four directions defined by these eight neighbors, i.e. 0, 45, 90, and 135 degrees. Define

$$M_g(i, j) = K_1 \sum_{d=0}^{3} |m_{ij}^{d\pi/4}|, \qquad (3-4)$$

where $m_{ij}^{d\pi/4}$, for $d = 0, \ldots, 3$ represents the slope information in these four directions. m_{ij}^0 corresponds to the horizontal slope m_{ij}^h and $m_{ij}^{\pi/2}$ the vertical slope m_{ij}^v of equation (3-3). The subscript g is used to indicate the generalized slope information at a pixel and K_1 is a constant used for scaling.

A thresholding operation is used to segment the range of values of the measure of spatial activity M_g such that the image will be divided into regions Ω_p, $p = 1, 2, \ldots, k$. The region Ω_p is chosen if

$$a_{p-1} < M_g(i, j) < a_p, \qquad (3-5)$$

where a_p is chosen subjectively depending on the range of M_g, the number of regions desired and the class of images being considered. The thresholds are chosen so that partitioning the image into regions is based either on equal segmentation of the range of M_g or more generally on an nonuniform segmentation of M_g. The nonuniform segmentation allows for more discrimination in heavily concentrated regions of spatial activity.

Once the image is divided into appropriate regions, the recursive filter is designed to meet the specifications of each region.

III.   A Scheme for Two-Dimensional Piecewise Recursive
       Estimation

Consider the following discrete image formation system: The image plane distribution function g which is the output of the system modeled in figure 1.1 is known. The input to the system is f, the object plane distribution function. The system is assumed to be linear with impulse response h. The output is added to a white, Gaussian noise to form g. The input-output equation is given by:

$$g(i,j) = \sum_{q=-\delta}^{\Theta} \sum_{m=-\gamma_q}^{\Gamma_q} h(q,m)f(i-q,j-m) + n(i,j), \qquad (3-6)$$

for $i = 0,1,\ldots,M-1$, $j = 0,1,\ldots,N-1$, $\delta,\Theta \geq 0$ shows the vertical extent of the blur, and γ_q, $\Gamma_q \geq 0$ the horizontal extent of the blur along the object horizontal line $i-q$. The image g is an MxN array of pixels. The problem at hand is in general one of inverse filtering, that is, given the output of the system g and the system impulse response h, to find an estimate of the input f.

In the method proposed in the present work, the model in figure 1.1 is modified slightly to account for the statistical nature of the object plane distribution function f. It is assumed that f is generated by passing white noise sources through a bank of linear systems, whose impulse responses are b_p for $p = 1,2,\ldots,k$, such that the object plane distribution function f is composed of a set of disjoint regions. Each of these regions is characterized by a zero-mean two-dimensional, stationary random field with a known autocorrelation function. This is depicted in figure 3-1. A difference equation model is developed for each region Ω_p, such that when the input is a white noise source the output of the system has statistics that match those of the pth region of f. Such a model is given by

$$\underline{z}_p(i,j+1) = Q_p\underline{z}_p(i,j) + S_p\underline{u}_p(i,j), \qquad (3-7)$$

$$f(i,j) = T_p\underline{z}_p(i,j), \qquad (3-8)$$
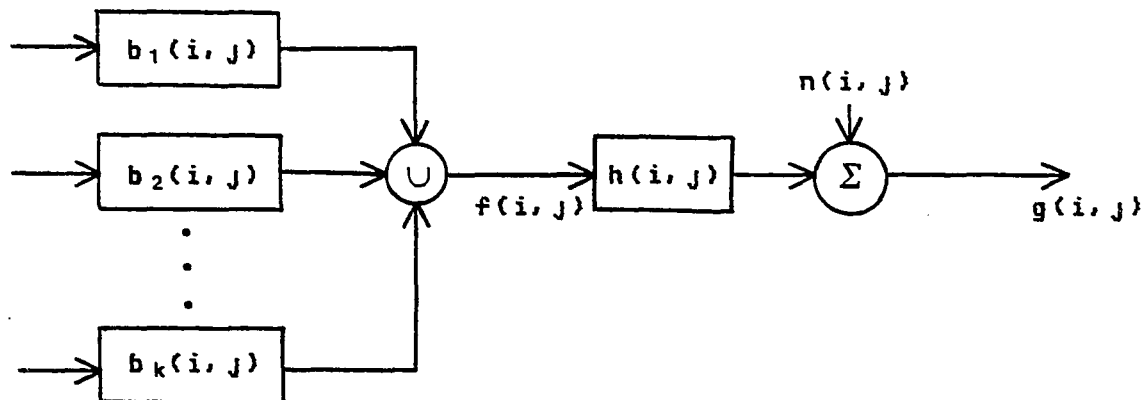
$b_k(i,j)$ — Linear system generating the object
distribution function $f(i,j)$ from a white
source at the input.

$f(i,j)$ — Object plane distribution function.

$h(i,j)$ — Image formation system impulse response.

$n(i,j)$ — Additive white noise source.

$g(i,j)$ — Received distorted image.

$\cup$ — Union of disjoint regions.

Figure 3.1

for $p = 1, 2, \ldots, k$, $i = 0, \ldots, M-1$, $j = 0, \ldots, N-1$, and where $E[\underline{u}(i, j)] = 0$ and $E[\underline{u}(i_1, j_1)\underline{u}(i_2, j_2)] = R_p \Delta(i_1 - i_2)\Delta(j_1 - j_2)$. The $E\{\underline{z}_p\} = 0$ and $E\{\underline{z}_p\underline{z}_p^T\} = K$.

Equation (3-6) defines the input-ouput relationship for the image formation system depicted in figure 3-1. It is necessary now to arrange equation (3-6) such that a difference equation model, such as described by equations (3-7) and (3-8) will result for the image formation system. In a manner similar to that of Aboutalib, et al. [1], the following development evolved.

Without loss of generality, it is assumed that $h(i, -\gamma_q) = 0$ for $-\delta \leq q \leq \theta$. Define, $\phi_q = \gamma_q + \Gamma_q$ and use the notation $r_{qm} = h(q, m-\gamma_q)$. Equation (3-6) now becomes,

$$g(i, j) = \sum_{q=-\delta}^{\theta} \sum_{m=0}^{\phi_q} r_{qm} f(i-q, j+\gamma_q-m) + n(i, j). \qquad (3-9)$$

If we introduce the shift operator $D^p f(i, j) = f(i, j-p)$, then the contribution to $g(i, j)$ from the object line $i-q$ is

$$g_q(i, j) = [r_{q0} + r_{q1} D+, \ldots, + r_{q\phi_q} D^{\phi_q}]$$
$$f(i-q, j+\gamma_q) + n(i, j). \qquad (3-10)$$

Now if we define,

$$H_q(D) = r_{q0} + r_{q1} D+, \ldots, + r_{q\phi_q} D^{\phi_q}, \qquad (3-11)$$

for $-\delta \leq q \leq \theta$, the total contribution from all the $\delta + \theta + 1$ lines

is

$$g(i, j) = \sum_{q=-\delta}^{\theta} H_q(D) f(i-q, j+\gamma_q) + n(i, j). \qquad (3\text{-}12)$$

Let, $L = \max \{\gamma_q; -\delta \leq q \leq \theta\}$ be equal to the maximum degree of anticipation of the blur over all the contributing lines. We may then define the following:

$$\underline{H}(D) = \text{col}[H_\theta(D) \; H_{\theta-1}(D) \; \ldots \; H_{-\delta}(D)] , \qquad (3\text{-}13)$$

the vector of causal moving average operator polynomials. Equation (3-12) can be written as

$$g(i, j) = \underline{H}^T(D)\underline{s}(i, j) + n(i, j), \qquad (3\text{-}14)$$

where the vector $\underline{s}(i, j)$ is now considered the input vector to the system and is defined by:

$$\underline{s}(i, j) = \text{col}[f(i-\theta, j+\gamma_\theta), f(i-\theta+1, j+\gamma_{\theta-1})$$
$$, \ldots, f(i+\delta, j+\gamma_{-\delta})], \qquad (3\text{-}15)$$

where $f(i, j)$ is defined by (3-7) and (3-8).

Since $\underline{H}^T(D)$ is a multi-input — single-output causal operator, it admits a recursive realization $(\widetilde{A}, \widetilde{B}, \widetilde{\underline{c}}^T, \widetilde{\underline{d}}^T)$ of the following form

$$\underline{x}(i, j+1) = \widetilde{A}\underline{x}(i, j) + \widetilde{B}\underline{s}(i, j), \qquad (3\text{-}16)$$

$$g(i, j) = \tilde{c}^T \underline{x}(i, j) + \tilde{\underline{d}}^T \underline{s}(i, j) + n(i, j), \qquad (3-17)$$

for $i = 0, 1, \ldots, M-1$, and $j = 0, 1, \ldots, N-1$. The white noise process is such that $E[n(i, j)] = 0$ and $E[n(i_1, j_1)n(i_2, j_2)] = \sigma^2 \Delta(i_1 - i_2) \Delta(j_1 - j_2)$. The dimension of A is the minimum order of all state-space realizations of $\underline{H}(D)$. The parameter matrices $A, B, \underline{c}^T, \underline{d}^T$ are either space-variant or constant depending on the nature of the degradation.

The degradation model described by (3-16) and (3-17) can be augmented with the object plane model (3-7) and (3-8), to yield the composite model for the entire system shown in figure 3-1.

$$\underline{w}_p(i, j+1) = A_p \underline{w}_p(i, j) + B_p \underline{u}_p(i, j), \qquad (3-18)$$

$$g(i, j) = \underline{c}_p^T \underline{w}_p(i, j) + n(i, j), \qquad (3-19)$$

for $p = 1, 2, \ldots, k$, $i = 0, \ldots, M-1$ and $j = 0, \ldots, N-1$. The noise source statistics are as given and the vector $\underline{w}_p^T(i, j) = [\underline{x}^T(i, j) \ \underline{z}_p^T(i, j)]$ is the state of the system with dimension defined by the dimension of $\underline{x}(i, j)$ and $\underline{z}_p(i, j)$. The matrices A_p, B_p, and $\underline{c}_p^T$ are determined as follows,

$$A_p = \begin{bmatrix} \tilde{A} & \tilde{B} \ T_p \\ 0 & Q_p \end{bmatrix} \qquad B_p = \begin{bmatrix} 0 \\ S_p \end{bmatrix} \qquad ,$$

$$\underline{c}^T = [\tilde{\underline{c}} \quad \tilde{\underline{d}}^T T_p \ ]. \qquad (3-20)$$

With the system model described in equations (3-18) and (3-19), it is desired to derive a class of optimal estimators which yield a linear function of the observation image as its estimate. From this model, we wish to find an estimate of the n vector $\underline{w}_p(i, j+1)$ denoted $\hat{\underline{w}}_p(i, j+1)$ which is a linear function of the observations $g(i,0), \ldots, g(i,j)$, and is constructed with least mean square error of the region Ω_p. This is accomplished by minimizing

$$E[\underline{w}_p(i, j+1) - \hat{\underline{w}}_p(i, j+1)]^T [\underline{w}_p(i, j+1) - \hat{\underline{w}}_p(i, j+1)]. \qquad (3-21)$$

We can write,

$$\underline{w}_p(i, j+1) = \alpha(i, j)\hat{g}(i, j), \qquad (3-22)$$

where $\alpha(i, j)$ is a (n x j+1) coefficient matrix and $\hat{g}(i, j)$ a (j+1)-vector of the observations $g(i,0), \ldots, g(i,j)$.

By substituting (3-22) into (3-21) and differentiating with respect to the elements of the matrix $\alpha(i, j)$ yields a set of equations:

$$E[\underline{w}_p(i, j+1) - \hat{\underline{w}}_p(i, j+1)]\hat{g}^T(i, m) = 0, \qquad (3-23)$$

for $m = 0, 1, \ldots, j$. This is commonly known as the orthogonality principle. It states that the linear estimate $\hat{\underline{w}}_p(i, j+1)$ which minimizes the quadratic cost given by (3-22)

is such that the estimation error $[\underline{w}_p(i, j+1) - \hat{\underline{w}}_p(i, j+1)]$ is uncorrelated with every observation $g(i, 0), \ldots, g(i, j)$.

The inverse filter that results from this formulation is the piecewise Kalman filter:

$$\hat{\underline{w}}_p(i, j | j) = [I - \beta_p(j)\underline{c}_p^T]A_p\hat{\underline{w}}_p(i, j-1 | j-1)$$

$$+ \beta_p(j)g(i, j), \tag{3-24}$$

$$\beta_p(j) = P_p(j)\underline{c}_p[\underline{c}_p^T P_p(j)\underline{c}_p + \sigma^2]^{-1}, \tag{3-25}$$

$$P_p(j+1) = A_p[I - \beta_p(j)\underline{c}_p^T]P_p(j)A_p^T + B_p R_p B_p^T, \tag{3-26}$$

for $p = 1, 2, \ldots, k$. The coefficient matrices A and B are the system coefficient matrices from equation (3-20) and $\underline{c}_p$ is the coefficient vector from (3-20). The vector $\beta_p(j)$ is the Kalman filter gain vector and $P_p(j)$ is the error covariance matrix for region k. The estimate of the input is derived from the estimate of the state vector by

$$\underline{s}(i, j) = [0 \ T_p]\hat{\underline{w}}_p(i, j | j), \tag{3-27}$$

where T is the parameter matrix from equation (3-7).

Equations (3-24) — (3-26) are the two-dimensional Kalman filtering equations for each region Ω_p. This filter is applied to the two-dimensional output signal g, and the output of the filter will be a best linear minimum mean square error estimate of the input signal f restricted to the region Ω_p.

The coefficient matrices in equations (3-24) — (3-26)

are specified in equation (3-20). The A, B, $\underline{c}^T$, $\underline{d}^T$ are determined by spectral factorization of the distortion modeled by the system impulse response h. These remain the same in each region. The coefficient matrices Q_p, T_p, S_p are dependent on the autocorrelation functions pertaining to each region Ω_p. It has been shown (Franks [9]) that for a stationary random process f the autocorrelation is

$$R(\tau) = A \sum_{m=0}^{\infty} r_m P(m,\tau), \qquad (3-28)$$

where $r_m = E[f_n f_{n+m}]$, and

$$A = E[f_n^2] \quad \text{and} \quad E[f_n] = 0.$$

$P(m,\tau)$ is the probability that points t and $t+\tau$ are in intervals m apart. If it assumed that $\{f_n\}$ is a wide-sense stationary sequence in the regions chosen then,

$$R_p(\tau,\sigma) = A_p \exp(-\lambda_{hp}|\tau| - \lambda_{vp}|\sigma|). \qquad (3-29)$$

The constant A_p is proportional to the variance and λ_{hp} and λ_{vp} specify the average number of statistically independent luminance levels in a unit distance along the horizontal and vertical directions. Alternatively, the correlation is characterized by the parameters $\rho_h = \exp[-\lambda_{hp} T_e]$ and $\rho_v = \exp[-\lambda_{vp} T_e]$ which are the correlation coefficients of the luminance levels of adjacent

picture elements when the picture area is quantized into small squares of dimension T_e. For our images $T_e = 1$ and the correlation coefficients can be calculated as,

$$\rho = \frac{\mu_{x_i x_{i+1}}}{\sigma^2} = \frac{E\{(x_i - \eta)(x_{i+1} - \eta)\}}{\sigma^2}. \qquad (3\text{-}30)$$

It has been pointed out that, in general, the assumption of wide-sense stationarity over the entire image is not true, but it will be seen that assuming regional wide-sense stationarity leads to significant improvement in the estimate. Once the autocorrelation functions of the regions are determined, the appropriate recursive filters can be designed using these autocorrelation functions and the appropriate weighting calculated for the additive noise.

It has been shown by Nahi and Franco [38] that under the assumption that the autocorrelation can be represented by equation (3-29), it is straightforward to obtain the coefficients Q, S, T in equations (3-7) - (3-8):

$$Q_p = -\lambda_{h_p}, \qquad (3\text{-}31)$$

$$S_p = (2^{-\lambda_{h_p}})^{1/2}, \qquad (3\text{-}32)$$

$$T_p T_p^T = \tilde{H}, \qquad (3\text{-}33)$$

where the kmth element of $\tilde{H}$ is $h_{km} = \exp(-\lambda_{vp}(m-k))$. The objective of this procedure is then to design regional Kalman filters based on the statistics of each of these regions.

IV. Visibility Adapted Observation Noise Model

We assume that the image formation system is contaminated by white Gaussian observation noise with zero mean and variance σ^2. Anderson and Netravali [2] and Netravali and Prasada [39] incorporated the visibility of the noise with respect to the human observer in the construction of their restoration filter. In what follows, we use a similar criterion in our restoration procedure.

We note that the use of the visibility criterion by the above authors was for the case in which the disturbance was caused by additive noise only. Our restoration procedure using the criterion takes into account, in addition to additive noise, the presence of motion blurs. The application of such a visibility function to the general image formation model is determined here.

The visibility function as derived by Anderson and Netravali [2] is a measure of the visiblity of the noise in an image to the human viewer. It is dependent on the amount of additive noise present as well as the masking function, which is the response of the human visual system to the spatial activity in the image. That is, at sharp transitions in image intensity, the contrast sensitivity of the human visual system decreases with the sharpness of the transition and increases exponentially as a function of the spatial distance from the transition. The masking function does indeed respond in such a manner, as is shown by

equation (3-2).

The following procedure, presented in more detail in chapter 2, is used for determining the form of the visibility function. First, the masking function $M_{kr}(\cdot,\cdot)$ is computed for each pixel (i,j); then a masking function value γ and a noise power V_n are chosen. To each pixel of the original image whose masking function M_{kr} is in the range $[\gamma - \Delta\gamma/2, \gamma + \Delta\gamma/2]$, where $\Delta\gamma$ is a small increment, white Gaussian noise of power V_{n_i} is added. For each value of M, three test images with noise powers V_{n_1}, V_{n_2}, V_{n_3} are generated.

A subjective test is performed under which the experimenter randomly selects a test image to which he adds just enough white noise to reach a point of subjective equivalence between the test image with noise power V_{n_i} and the image with additive white noise of power V_{w_i}. The result of these tests is the visibility function given in equation (2-37) and quoted below

$$V(\gamma) = \frac{1}{\Delta\gamma} \frac{V_{w_1} + V_{w_2} + V_{w_3}}{V_{n_1} + V_{n_2} + V_{n_3}} . \qquad (3-34)$$

The resulting curves which express a relationship between the visibility of the noise and the masking value as published by Anderson and Netravali [2] have the general form of

$$V(M_{kr}(i,j)) = A_1 exp(-k_1 M_{kr}(i,j)), \quad for \ 0 \leq M_{kr}(i,j) \leq P \quad (3-35)$$

$$A_2 exp(-k_2 M_{kr}(i,j)), \quad for \ P < M_{kr}(i,j) \quad (3-36)$$

where k_1 and k_2 are constants dependent on the slopes of the curves and P is an appropriate positive constant.

Recall the piecewise Kalman filtering equations (3-24) - (3-26). The statistics of the noise are utilized in (3-25) in determining the amplification factor for the filter. The variance σ^2 of the noise is the term that represents the additive noise present in the system. In what follows, it is weighted by the visibility function to adjust the restoration filter according to the visibility of the noise by the human observer.

First, the visibility function is scaled so that in areas of no spatial activity, i.e. where the masking function is equal to zero, the variance of the noise is exactly equal to σ^2. In such regions, the human eye is most sensitive to additive noise; therefore as much noise as possible is removed. In a region of high spatial activity, the relative visibility of the noise is less than one. In these regions the filter can pass more noise until its subjective visibility is equal to that in the spatially inactive regions. The noise variance becomes

$$\sigma^2(i,j) = \sigma_N^2 / V(M_{kr}(i,j)). \quad (3-37)$$

The result is that the piecewise Kalman filtering equations

now adapt to the noise as observed by the human receiver, and according to (3-37) this variance depends nonlinearly on the state. Hence, even though we use the basic Kalman filter equations, the overall filter structure is piecewise and nonlinear.

There is one significant problem with the utilization of the above procedure as it stands. Since it is assumed that only the distorted image is available for use, it is true and is indicated by Anderson and Netravali [2], that there is a marked reduction in the quality of the restored image when the masking function is determined from an already noisy image. This problem is overcome in the present work by the development of a difference estimation operator to be used in the calculation of the slopes in the masking function. The difference estimation operator for the one-dimensional case is,

$$\widetilde{D}(x) = \frac{1}{w_1} \sum_{u=x}^{x+w_1} g(u) - \frac{1}{w_2} \sum_{u=x-w_2}^{x} g(u). \qquad (3-38)$$

This operator windows lengths w and w just before and after x, then averages g over the windows and takes the difference of the averages. This provides us with a more accurate measurement of the slope in a noisy image. For the two-dimensional case the directional difference estimation operators can be defined as,

$$\widetilde{D}_v(x_1, x_2) = \frac{1}{w_1} \sum_{u=x_2}^{x_2+w_1} g(x_1, u) - \frac{1}{w_2} \sum_{u=x_2-w_2}^{x_2} g(x_1, u), \qquad (3-39)$$

$$\widetilde{D}_h(x_1, x_2) = \frac{1}{v_1} \sum_{u=x_1}^{x_1 + v_1} g(u, x_2) - \frac{1}{v_2} \sum_{u=x_1-v_2}^{x_1} g(u, x_2), \quad (3-40)$$

where w_1, w_2 and v_1, v_2 define the extents of the window in the vertical and horizontal direcions, respectively. In general this difference estimation operator can be used to determine the slope information in any direction.

V. Determination of the Previous State Vector by a Nearest Neighbor Criterion

The adaptive nonlinear Kalman-type filtering equations as derived in section III are given by,

$$\underline{\hat{w}}_p(i, j \mid j) = [I - \underline{g}_p(j)\underline{c}_p^T]A_p\underline{\hat{w}}_p(i, j-1 \mid j-1)$$

$$+ \underline{g}_p(j)g(i, j), \qquad (3-41)$$

$$\underline{g}_p(j) = P_p(j)\underline{c}_p[\underline{c}_p^T P_p(j)\underline{c}_p + \sigma^2]^{-1}, \qquad (3-42)$$

$$P_p(j+1) = A_p[I - \underline{g}_p(j)\underline{c}_p^T]P_p(j)A_p^T + B_p R_p B_p^T. \qquad (3-43)$$

A problem can still exist in the implementation stage of the procedure. In each region, the Kalman filter is implemented so that the current pixel (i, j) is dependent on the state vector of pixel $(i, j-1)$. At the boundary between two regions this can lead to poor results. Pixel $(i, j-1)$ may be in a region characterized by significantly different statistical information. This is seen by the illustration in figure 3-2.
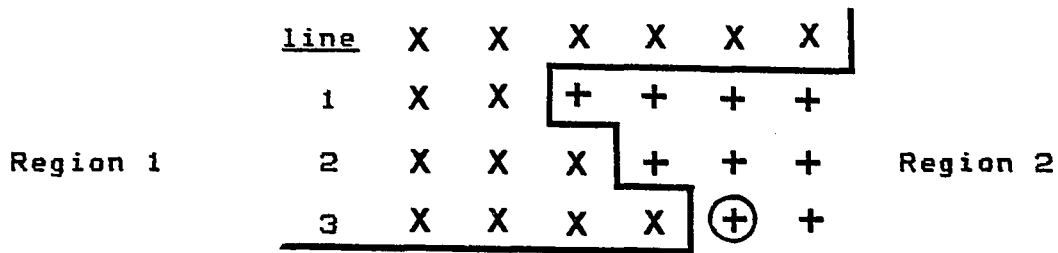
Figure 3-2

Consider the x's to denote pixels in one region and the +'s to denote pixels in a second region. If scanning is being done on row 3 and an estimate is being calculated for the circled pixel, the previous state for $\oplus$ is in the other region. If the autocorrelation function for region 1 is significantly different than the autocorrelation function for region 2 this leads to a poor estimate for the state vector of $\oplus$. In this case, it would be desirable to determine which one of its other neighbors would be better suited for the previous state.

The second case where better previous state information may be needed is in regions of high spatial activity. There are two possible explanations for this result. Since the image to which one has access is a degraded image, some of the significant edge information may be lost by the degradation process. It is possible that edges are smoothed to such an extent that these areas appear to have a lower amount of spatial activity than actually exists. Secondly,

it is possible that in regions of high spatial activity an autocorrelation function of a different form than shown in (3-34) should be used. In either case, use of a nearest neighbor criterion to choose the best previous state improves the quality of the restored image.

It is proposed that under these two conditions one should consider all of a pixel's previously processed closest neighbors when determining which pixel should be used as its previous state. The neighborhood to which a pixel belongs is defined as those points surrounding the pixel encased by any m x n window. In each region the Kalman filter is implemented in whichever manner one chooses, i.e. left to right, top to bottom, etc. Note that the implementation procedure tends to bias the estimation in one direction, therefore it may be desirable to scan in the reverse direction in a second pass. For the purposes of this development it is assumed that the Kalman filter is implemented from left to right and the previous state for pixel (i, j) will be obtained from pixel (i, j-1). However, in regions of high spatial activity or at the boundary of two regions, each pixel in the desired neighborhood will be checked. As an example choose a 3 x 3 neighborhood. It is shown in figure 3-3 that there are four pixels in this neighborhood whose state vector has previously been estimated.

```
X    X    X

X    +
```

Figure 3-3

For pixel + at (i,j) the four nearest neighbors for which
state vectors have been previously calculated are $(i,j-1)$,
$(i-1,j-1)$, $(i-1,j)$, and $(i-1,j+1)$. Note, that as shown in
figure 3-4 it is possible for a given pixel, denoted 1, to
be he previous state for the next pixel in row 2 and for
pixel 2 in row 3. In this eventuality the two paths from 1
do not intersect. In fact, it is clear that this procedure
generates a tree of pixels whose vertices are certain pixels
and the edges are strings of subsets of the remaining
pixels.

Line

```
1    X    X    X    X

2    X    X    +₁   +

3    X    X    X    +₂
```

Figure 3-4

In regions of high spatial activity, one expects to see relatively large differences in intensity values. If, for one of the reasons previously mentioned, the autocorrelation information is not exact, the adaptive nonlinear Kalman-type filter may not be able to follow these changes in intensity. For this reason, it is desirable to choose that neighbor which most closely matches the pixel in intensity and spatial activity.

The fundamental question now becomes one of how to choose the nearest neighbors for the previous state information. On what criterion is similarity measured from one pixel to another? The criterion function used for the nearest neighbor decision will be based on the spatial activity information of the pixel's neighbors as well as the intensity levels. This is natural because the property with which each region was originally classified was determined by the amount of spatial activity. In addition, it is important to also maintain a consistency in the intensity levels. This is of considerable importance at the edge of a region where there is a significant difference between gray levels on either side of the edge. Any of a number of measures of similarity could be used to determine a pixel's nearest neighbor. Define the similarity measure as Ψ, then all of the following are possible measures:

(1). $\Psi_1(f(i,j),f(i',j')) = |f(i,j) - f(i',j')|^2$
$$+ |M_g(i,j) - M_g(i',j')|^2. \qquad (3\text{-}45)$$

(2). $\Psi_2(f(i,j),f(i',j')) = |M_g(i,j) - M_g(i',j')|^2$.   (3-46)

(3). $\Psi_3(f(i,j),f(i',j')) = K_2|f(i,j)M_g(i,j)$

$$- f(i',j')M_g(i',j')|, \qquad (3-47)$$

where M_g is the spatial activity at pixel (i,j) as given by equation (3-4). The first two functions Ψ are metric distance measures between two pixels. Ψ_1 is a measure of the distance in slope information and the intensity between two. pixels, while Ψ_2 is a measure of the distance with respect to slope only. Ψ_3 is a measure of the difference in product of the slope information and intensity between two pixels. This is the measure chosen in the present work in the application of the nearest neighbor criterion. The measure Ψ_3 can be interpreted from the following point of view

$$|\nabla(f^2(x,y))| = 2f(x,y)((\partial f(x,y)/\partial x)^2 + (\partial f(x,y)/\partial y)^2)^{1/2}. \quad (3-48)$$

Ψ_3 is therefore a measure of the slope of the intensity function squared. This indicates that in regions of high intensity the slope information is more heavily weighted than in regions of low intensity.

The resulting adaptive nonlinear Kalman-type filtering equations are

$$\hat{\underline{w}}_p(i, j | j) = [I - \phi_p(j)\underline{c}_p^T]A_p\hat{\underline{w}}_p(i*, j*| j*)$$

$$+ \phi_p(j)g(i, j), \tag{3-49}$$

$$\phi_p(j) = P_p(j)\underline{c}_p[\underline{c}_p^T P_p(j)\underline{c}_p + \sigma^2]^{-1}, \tag{3-50}$$

$$P_p(j+1) = A_p[I - \phi_p(j)\underline{c}_p^T]P_p(j)A_p^T + B_p R_p B_p^T, \tag{3-51}$$

for $p = 1, 2, \ldots, k$ and $(i*, j*)$ is the position of the pixel that is used for the previous state information. A block diagram of the whole system is shown in figure 3-5.

VI. Interpolation Procedure for Initial State Determination

The final question that arises is, how can the estimates of the initial points of a region be improved if insufficient initial condition information is available? The problem is compounded if there are a great number of regions and no a priori information about the initial states.

The solution proposed for improving the initial estimate in each region is by implementing a two-dimensional interpolation scheme for the initial points in a region. Consider the following model:

$$\underline{w}(i, j+1) = A\underline{w}(i, j) + B\underline{u}(i, j), \tag{3-52}$$

$$g(i, j) = \underline{c}^T\underline{w}(i, j) + dn(i, j). \tag{3-53}$$

It is assumed that scanning will be done across each row with the observations $g(i, m)$ for $m = 0, 1, \ldots, j$ given. The
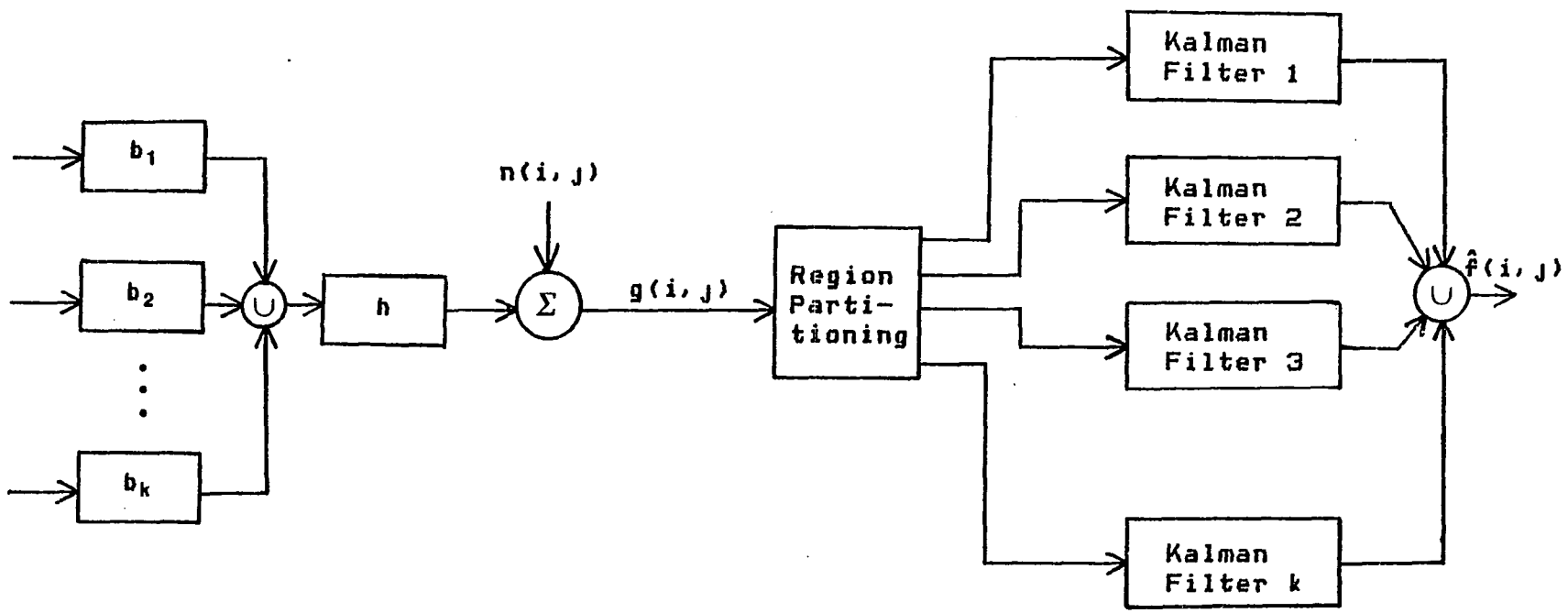
Figure 3.5

problem is to determine the best linear estimate of $\underline{w}(i,j-p)$ for $p>0$. Let us denote the estimate of $\underline{w}(i,j-p)$ as $\hat{\underline{w}}(i,j-p|j)$. The problem of finding the best linear estimate of $\underline{w}(i,j-p)$ is one of determining the set of constants $a(i,m)$ for $m = 0,1,\ldots,j$ such that:

$$\hat{\underline{w}}(i,j-p|j) = a(i,m)\hat{g}(i,m),\qquad\qquad (3-54)$$

which minimize the cost function:

$$E[\underline{w}(i,j-p) - \hat{\underline{w}}(i,j-p|j)]^T Q[\underline{w}(i,j-p) - \hat{\underline{w}}(i,j-p|j)].\quad (3-55)$$

for any positive definite matrix Q. If we substitute (3-54) into (3-55) the result is,

$$E[\underline{w}(i,j-p) - a(i,m)\hat{g}(i,m)]^T Q$$
$$[\underline{w}(i,j-p) - a(i,m)\hat{g}(i,m)].\qquad\qquad (3-56)$$

Minimization of (3-56) requires differentiating (3-56) with respect to the constants $a(i,j)$ and setting the resultant equal to zero. This yields the following equations.

$$E[\underline{w}(i,j-p) - \hat{\underline{w}}(i,j-p|j)]\hat{g}^T(i,m) = 0,\qquad\qquad (3-57)$$

for $m = 0,1,\ldots,j$. As in the one-dimensional case this equation may be interpreted as an orthogonality condition.

In a fashion comparable to that in two-dimensional Kalman filtering, we would like to find a recursive technique for implementing the interpolation scheme. The recursive formula for interpolation is given by,

$$\underline{\hat{w}}(i, j-p \mid j) = K \; \underline{\hat{w}}(i, j-p+1 \mid j) + L \; \underline{\hat{w}}(i, j-p+1).$$ (3-58)

In equation (3-58), $\underline{\hat{w}}(i, j-p+1)$ is the one-step prediction of $\underline{w}(i, j-p+1)$ using the observations $g(i, m)$, $m = 0, 1, \ldots, j-p$, with $\underline{\hat{w}}(i, j-p+1)$ the optimal previous state, and $\underline{w}(i, j-p+1 \mid j)$ is the $j-1$ optimal interpolation given $g(i, m)$, $m = 0, 1, \ldots, j-p$. We now need to find the necessary constants K and L to satisfy (3-56). If we substitute (3-58) into (3-57) we get,

$$E[\underline{w}(i, j-p) - K \; \underline{\hat{w}}(i, j-p+1 \mid j)$$
$$- L \; \underline{w}(i, j-p+1)]\hat{g}^T(i, m) = 0,$$ (3-59)

for $m = 0, 1, \ldots, j$. Since $\underline{\hat{w}}(i, j-p+1 \mid j)$ is assumed to be the optimal estimate of $\underline{w}(j-p+1)$ given $g(i, m)$, $m = 0, 1, \ldots, j$, then it must satisfy (3-57). Now, substitute this into (3-59).

$$E[\underline{w}(i, j-p) - K \; \underline{w}(i, j-p+1)$$
$$- L \; \underline{\hat{w}}(i, j-p+1)]\hat{g}^T(i, m) = 0,$$ (3-60)

for $m = 0, 1, \ldots, j$. In order to solve for the coefficients K

and L consider the original system formulation in (3-53). If it is assumed that A is a nonsingular matrix (3-60) becomes:

$$E[A^{-1} \underline{w}(i, j-p+1) - A^{-1} B\underline{u}(i, j-p) - K \underline{w}(i, j-p+1)$$

$$- L \hat{\underline{w}}(i, j-p+1)]\hat{g}^T(i, m) = 0, \quad m = 0, \dots, j. \quad (3-61)$$

Now if we make a change of variables, $\tilde{\underline{w}} = \underline{w} - \hat{\underline{w}}$, and then add and subtract the term $[A^{-1} - K]\hat{\underline{w}}(i, j-p+1)$ to (3-60) the result is,

$$E\{[A^{-1} - K]\tilde{\underline{w}}(i, j-p+1) + [A^{-1} - K - L]\hat{\underline{w}}(i, j-p+1)$$

$$- A^{-1} B\underline{u}(i, j-p)\}\hat{g}^T(i, m) = 0, \quad m = 0, \dots, j. \quad (3-62)$$

Since we know that $\hat{\underline{w}}(i, j-p+1)$ is the one-step prediction of $\underline{w}(i, j-p+1)$ using observations $g(i, m)$, $m = 0, \dots, j-p$ and that $\hat{\underline{w}}(i, j-p+1|j)$ is the $j-1$ optimal interpolation given $g(i, m)$, $m = 0, \dots, j-p$, consider dividing (3-62) into two parts. One part for $m = 0, \dots, j-p$ and the other part for $m = j-p+1, \dots, j$. First take $m = 0, \dots, j-p$,

$$E[(A^{-1} - K)\tilde{\underline{w}}(i, j-p+1) + [A^{-1} - K - L]\hat{\underline{w}}(i, j-p+1)$$

$$- A^{-1} B\underline{u}(i, j-p)]\hat{g}^T(i, m) = 0, \quad m = 0, \dots, j-p. \quad (3-63)$$

By definition $\hat{\underline{w}}(i, j-p+1)$ is the optimal estimate given the observations $g(i, 0), \dots, g(i, j-p)$. Using the fact that $\underline{u}(i, j-p)$ is independent of $g(i, m)$ for $m = 0, 1, \dots, j-p$, and

equation (3-57) results in the following relationship,

$$A^{-1} - K - L = 0. \qquad (3-64)$$

Now consider (3-62) for $m = j-p+1, \ldots, j$,

$$E[A^{-1} - K]\widetilde{\underline{w}}(i, j-p+1)$$
$$- A^{-1}B\underline{u}(i, j-p)]\hat{\underline{g}}^T(i, m) = 0. \qquad (3-65)$$

First, take the case when $m = j-p+1$. From (3-65) and (3-53),

$$E\{[A^{-1} - K]\widetilde{\underline{w}}(i, j-p+1) - A^{-1}B\underline{u}(i, j-p)\}$$
$$\cdot[\underline{c}^T\underline{w}(i, j-p+1) + d\ n(i, j-p+1)]^T = 0. \qquad (3-66)$$

We know n is independent of $\widetilde{\underline{w}}$ and $\underline{u}$, and since $\hat{\underline{w}}$ is a linear combination of $g(i, j)$,

$$E\{[A^{-1} - K]\widetilde{\underline{w}}(i, j-p+1)\}\underline{w}^T(i, j-p+1)\underline{c}$$
$$- E\{[A^{-1}B\underline{u}(i, j-p)\hat{\underline{w}}^T(i, j-p+1)\underline{c}] = 0. \qquad (3-67)$$

If we let, $E[\underline{w}(i, j)\underline{w}^T(i, j)] = P(i, j)$, then

$$[A^{-1} - K]P(i, j-p+1)\underline{c}$$
$$- E[A^{-1}B\underline{u}(i, j-p)\underline{w}^T(i, j-p+1)\underline{c}] = 0. \qquad (3-68)$$

From (3-52) and knowing that $\underline{u}$ is independent of $\underline{w}$ and

$$E[\underline{u}(i, j-p)\underline{w}^T(i, j-p+1) = RB^T,$$

$$\{[A^{-1} - K]P(i, j-p+1) - A^{-1}BRB^T\}\underline{c} = 0. \qquad (3-69)$$

Now take,

$$K = \Phi(j-p). \qquad (3-70)$$

(3-70) is now satisfied when

$$\Phi(j) = A^{-1}[I - BRB^TP^{-1}(i, j+1)]. \qquad (3-71)$$

If (3-70) is true then it will be shown that (3-56) will hold for m = j-p+2,....,j. From (3-70) and (3-71),

$$A^{-1} - K = A^{-1}BRB^TP^{-1}(i, j-p+1). \qquad (3-72)$$

Substituting (3-72) into (3-65) requires that,

$$E\{[A^{-1}BRB^TP^{-1}(i, j-p+1)\underline{w}(i, j-p+1)$$
$$- A^{-1}B\underline{u}(i, j-p)\}g^T(i, j) = 0, \qquad (3-73)$$

for m = j-p+1,....,j. Now choose any value of m such as k so that j-p+1 $\leq$ k $\leq$ j. Then,

$$g(i, m) = \underline{c}^T\underline{w}(i, m) + d\ n(i, m). \qquad (3-74)$$

If equation (3-53) is solved for $\underline{w}(i,m)$ with initial conditions equal to $\underline{w}(i,j-p+1)$ the result is,

$$\hat{\underline{w}}(i,m) = N\underline{w}(i,j-p+1) + F[\underline{u}(i,m)], \quad \text{for } m \geq j-p+1, \quad (3-75)$$

where $F[\cdot]$ is some function of $\underline{u}(i,m)$. Therefore (3-73) becomes,

$$E[BRB^T P^{-1}(i,j-p+1)\underline{w}(i,j-p+1)\underline{w}^T(i,j-p+1)N^T\underline{c}]$$
$$- E[B\underline{u}(i,j-p)\underline{w}^T(i,j-p+1)N^T\underline{c}] = 0. \quad (3-76)$$

If we summarize these results, we have,

$$\hat{\underline{w}}(i,j-p|p) = \Phi(i,j-p)\hat{\underline{w}}(i,j-p+1|j)$$
$$+ [A^{-1} - \Phi(i,j-p)]\hat{\underline{w}}(i,j-p+1). \quad (3-77)$$

and

$$\Phi(i,j) = A^{-1}[I - BRB^T P^{-1}(i,j+1)]. \quad (3-78)$$

It should be noted that during the recursive estimation procedure, estimates $\hat{\underline{w}}(j-p+1)$ were determined along with the values of $P(i,j-p+1)$. It will be necessary to store these values to perform the interpolation.

VII. Conclusions

The nonlinear adaptive recursive estimation procedure is implemented by the two-dimensional Kalman filtering equations represented by:

$$\hat{\underline{w}}_p(i,j|j) = [I-\phi_p(j)\underline{c}_p^T]A_p\hat{\underline{w}}_p(i*,j*|j*)$$

$$+ \phi_p(j)g(i,j), \tag{3-80}$$

$$\phi_p(j) = P_p(j)\underline{c}_p[\underline{c}_p^T P_p(j)\underline{c}_p + \sigma^2]^{-1}, \tag{3-81}$$

$$P_p(j+1) = A_p[I - \phi_p(j)\underline{c}_p^T]P_p(j)A_p^T + B_p R_p B_p^T, \tag{3-82}$$

where $(i*,j*)$ is used to denote the position of the pixel that is used for the previous state information. The coeffients A_p, B_p, $\underline{c}_p^T$ are chosen to match the model of the object distribution function and the degradation as described by the image formation system. These coefficients will be either constant or time-varying depending on the type of distortion present. The variance of the observation noise σ^2 is adapted at each pixel to account for the response of the human visual system to this noise. This causes the Kalman filtering equations to be nonlinear in each region. A nearest neighbor test is done prior to updating equation (3-80) to determine which of the neighbors of a pixel should be used for the previous state information. In addition, if insufficient knowledge of the initial state is known then the two-dimensional interpolation scheme is implemented to obtain this

information.

CHAPTER 4

EXPERIMENTAL RESULTS

I. Problem Formulation

The adaptive nonlinear Kalman-type filtering equations for two-dimensional signals are given by:

$$\hat{\underline{w}}_p(i, j \mid j) = [I - \phi_p(j)\underline{c}_p^T]A_p\hat{\underline{w}}_p(i*, j* \mid j)$$

$$+ \phi_p(j)g(i, j), \tag{4-1}$$

$$\phi_p(j) = P_p(j)\underline{c}_p[\underline{c}_p^T P_p(j)\underline{c}_p + \sigma^2]^{-1}, \tag{4-2}$$

$$P_p(j+1) = A_p[I - \phi_p(j)\underline{c}_p^T]P_p(j)A_p^T + B_p R_p B_p^T. \tag{4-3}$$

where $p = 1, 2, \ldots, k$. The coefficient matrices A_p, B_p , R_p and $\underline{c}_p$ are dependent on the structure of the image formation system being modeled and $(i*, j*)$ represents the position of the pixel used for the previous state information. The general procedure for the implementation of this restoration is described below.

An Adaptive Nonlinear Kalman-Type Filtering Algorithm

Step 1. Calculate the masking function for
         each image using equation (3-19).

Step 2. Divide the image into regions using the
         directional derivative information given by

(3-24) through (3-25).

Step 3. Determine the statistical information

for each region according to (3-36).

    a. Horizontal correlation coefficient, α_p.

    b. Vertical correlation coeffficient, β_p.

Step 4. Using this statistical information calculated

in step 3 and known information about the point

spread function determine the Kalman filtering

coefficients A_p, B_p, $\underline{c}_p^T$.

Step 5. Implement the regional Kalman filtering scheme.

    a. At each line i, scan line $i+1$ to determine

which state vector and error covariance

matrices are to be saved and used as the

previous state information in line i. This

is done by using the nearest-neighbor

criterion in equation (3-43).

    b. If there is a lack of initial condition

information, implement the interpolation

scheme on the initial points in each region.

The implementation of this adaptive nonlinear Kalman-type filter was performed on a DEC PDP 11/55 computer. A GENISCO Color Graphics Display System, supported by this computer, was used to display the digitized images. All the images used were previously digitized and contained 256 picture elements per line and 256 lines per frame. The data bases for the images in figure 4-1c and 4-1d were obtained

from Bell Laboratories, Holmdel, New Jersey.

The form of the autocorrelation function on each region p is

$$R(\tau, \sigma) = A_p \exp[-\lambda_{h_p}|\tau| - \lambda_{v_p}|\sigma|], \qquad (4-4)$$

for $p = 1, 2, \ldots, k$. Each A_p, λ_{h_p}, λ_{v_p} are determined in step 3 of the algorithm. The model for the distortion used was consistent with that of Aboutalib, et al. [1]. The distortion is a model of the combination of horizontal translation and vertical oscillatory vibration. This is one of the many possible types of motion that occur in imaging systems. The horizontal translation is assumed to have an extent of H pixels and the vertical vibration affects V lines. The model for this type of distortion is given by

$$g(i, j) = \sum_{k=0}^{H-1} \sum_{m=0}^{V} h(k, m) f(i-k, j-m) + n(i, j). \qquad (4-5)$$

The values of V and H used in the simulations are H = 5 and V = 2. It is also assumed that h(k, m) = 1 for k = 0, 1 and m = 0, ..., 5. Equation (4-5) now becomes

$$g(i, j) = \sum_{k=0}^{1} \sum_{m=0}^{5} f(i-k, j-m) + n(i, j). \qquad (4-6)$$

The noise is white, Gaussian with a mean of zero and a standard deviation of 14.142.

Recall that the difference equations for the image formation system are given by

$$\underline{x}(i, j+1) = \widetilde{A}\underline{x}(i, j) + \widetilde{B}\underline{s}(i, j), \qquad (4-7)$$

$$g(i, j) = \widetilde{\underline{c}}^T\underline{x}(i, j) + \widetilde{\underline{d}}^T\underline{s}(i, j) + n(i, j). \qquad (4-8)$$

The coefficient matrices $\widetilde{A}$, $\widetilde{B}$, $\widetilde{\underline{c}}^T$, $\widetilde{\underline{d}}^T$ are determined from the equation (4-6)

$$\widetilde{A} = \begin{bmatrix} 0 & -1 & -1 & -1 & -1 \\ 0 & 0 & 0 & 0 & 0 \\ 0 & 1 & 0 & 0 & 0 \\ 0 & 0 & 1 & 0 & 0 \\ 0 & 0 & 0 & 1 & 0 \end{bmatrix}$$

$$\widetilde{B} = \begin{bmatrix} 1 & -1 & 0 & 0 & 0 \\ 1 & -1 & 0 & 0 & 0 \end{bmatrix}$$

$$\widetilde{\underline{c}}^T = \begin{bmatrix} 1 & 0 & 0 & 0 & 0 \end{bmatrix} \text{ and } \widetilde{\underline{d}}^T = \begin{bmatrix} 1 & 1 \end{bmatrix}.$$

The difference equations that represent the object distribution function formation are:

$$\underline{z}_p(i, j+1) = Q_p\underline{z}_p(i, j) + S_p\underline{u}_p(i, j), \qquad (4-9)$$

$$\underline{f}(i, j) = T_p\underline{z}_p(i, j), \qquad (4-10)$$

for $p = 1, 2, \ldots, k$. The resulting coefficient matrices Q,

S , T are determined from the values of A_p, λ_{h_p} , λ_{v_p} in equation (4-4).

$$Q = \exp(-\lambda_{h_p}), \qquad (4-11)$$

$$S = [2^{-\lambda_{h_p}}] \quad , \qquad (4-12)$$

$$T_p T_p^T = \widetilde{H}, \qquad (4-13)$$

where the elements of $\widetilde{H}$ are determined by $h_{km} = \exp(- \lambda_{v_p} (k-m))$. The composite model dynamic equations are,

$$\underline{w}_p(i, j+1) = A_p \underline{w}_p(i, j) + B_p \underline{u}_p(i, j), \qquad (4-14)$$

$$g(i, j) = \underline{C}_p \underline{w}_p(i, j) + n(i, j), \qquad (4-15)$$

for p = 1,2,...,k. The coefficients for these composite equations are calculated from the following relationships

$$A_p = \begin{bmatrix} \widetilde{A} & \widetilde{B} \; T_p \\ 0 & Q_p \end{bmatrix} \quad B_p = \begin{bmatrix} 0 \\ S_p \end{bmatrix}$$

$$\underline{C}_p = \begin{bmatrix} \widetilde{c}^T & \widetilde{\underline{d}}^T T_p \end{bmatrix}. \qquad (4-16)$$

The coefficients in (4-16) are from equations (4-9), (4-10), (4-14), and (4-15).

In the masking function given by equation (3-2), the constant C = 0.35 and k = r = 1. The resulting form of the masking function is,

$$M_{kr}(i, j) = \sum_{p=i-1}^{i+1} \sum_{q=j-1}^{j+1} 0.35^{\|(i, j)-(p, q)\|} [\,|m_{ij}^v|+|m_{ij}^h|\,]. \quad (4-17)$$

Several different classes of images were chosen to test the validity of the proposed image restoration scheme. The representative of the first class of images is a simple diagonal two-tone image shown in figure 4-1a. Figure 4-1b is the same image zoomed up by a factor of four to allow closer examination of the effect of the distortion. The zoom was performed on the upper left corner of figure 4-1a. The second class of images is represented by the woman shown in figure 4-1c. The final class is that of written text and is exemplified in figure 4-1d.
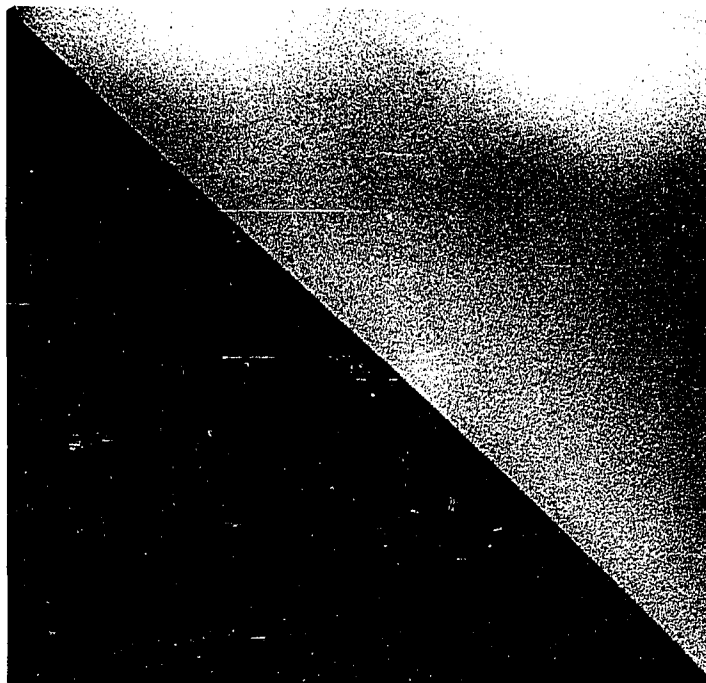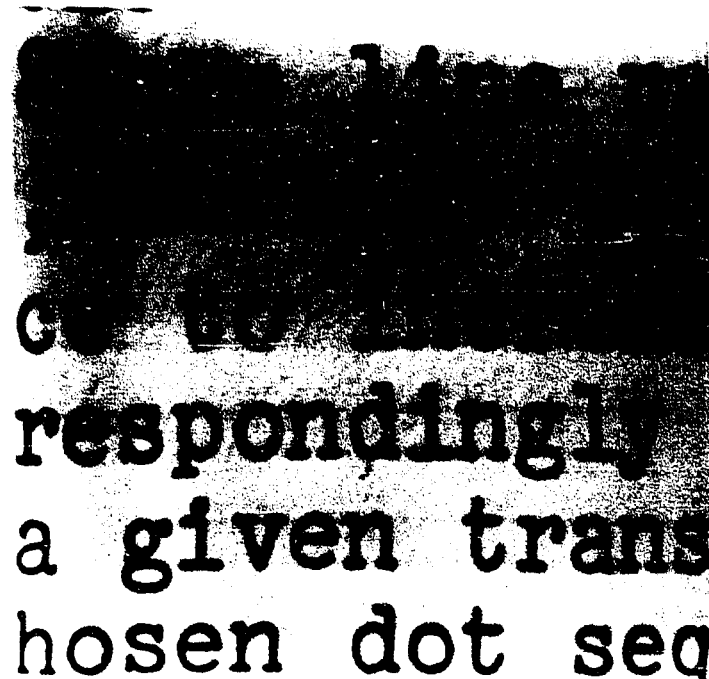

(a)
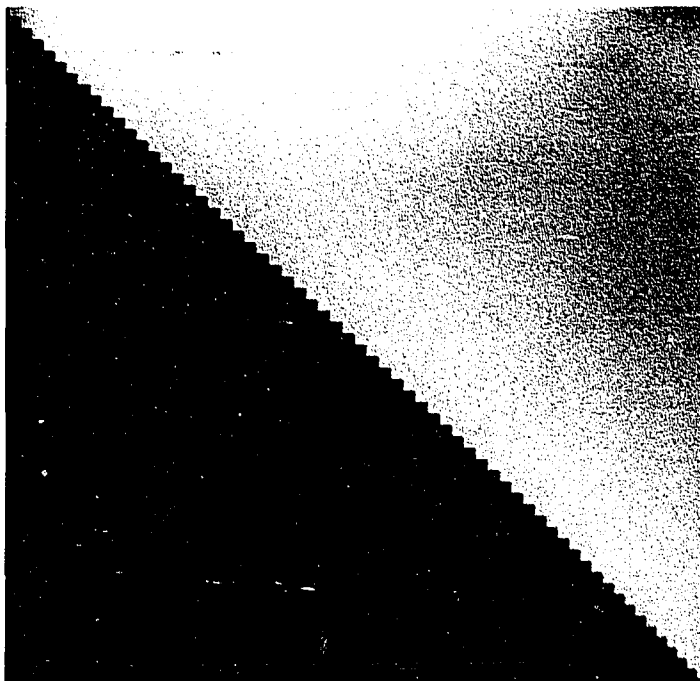
(b)

(c)

(d)

Figure 4-1. Original pictures. The original pictures are 256x256 arrays of discrete points with each pixel linearly quantized to 8 bits. The variance of each image is: (a) $\sigma^2 = 2232$, (c) $\sigma^2 = 2694$, and (d) $\sigma^2 = 685$.

The images of figure 4-1 were degraded using the distortion described in equation (4-6) and the noise added was white, Gaussian noise with a standard deviation of 14.142. The degraded images are shown in figures 4-2a, 4-2b, 4-2c, and 4-2d. Again, the second image in figure 4-2

is zoomed by a factor of four. The degradation is clearly
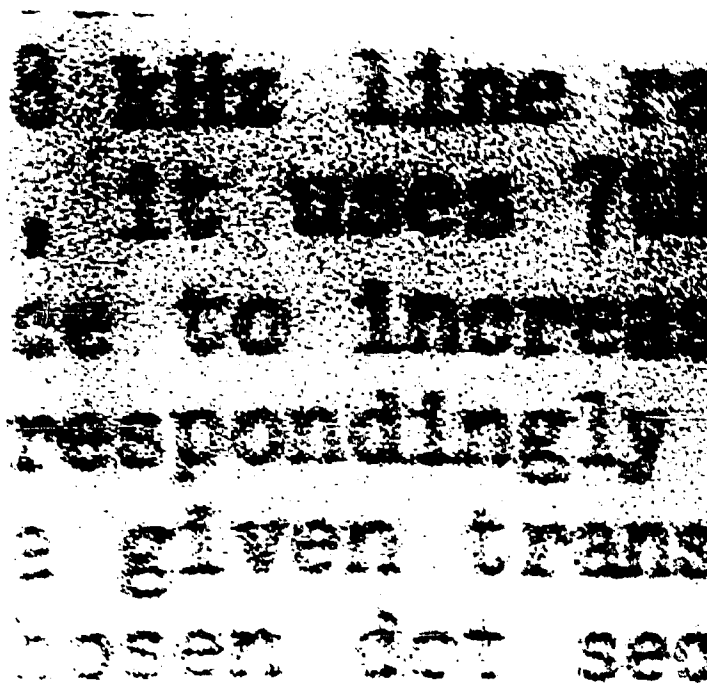seen in the zoomed portion of the image.
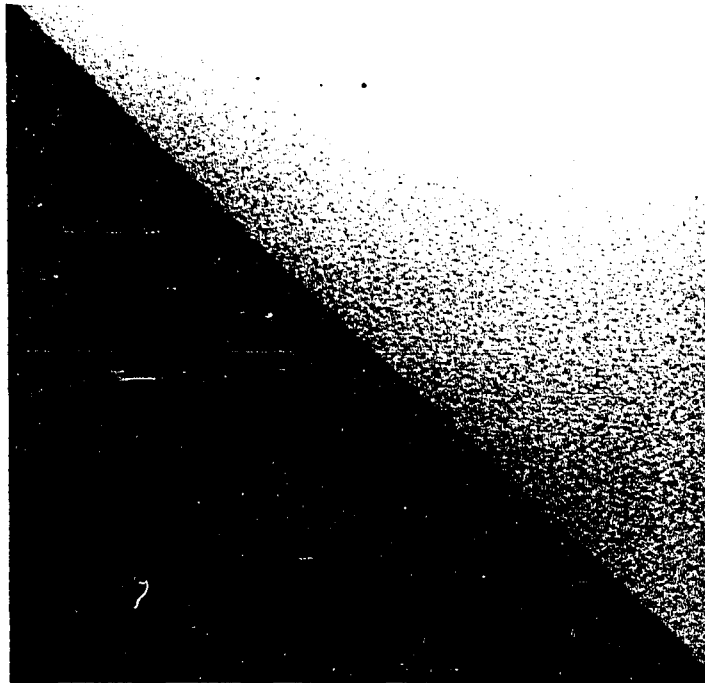
(a)
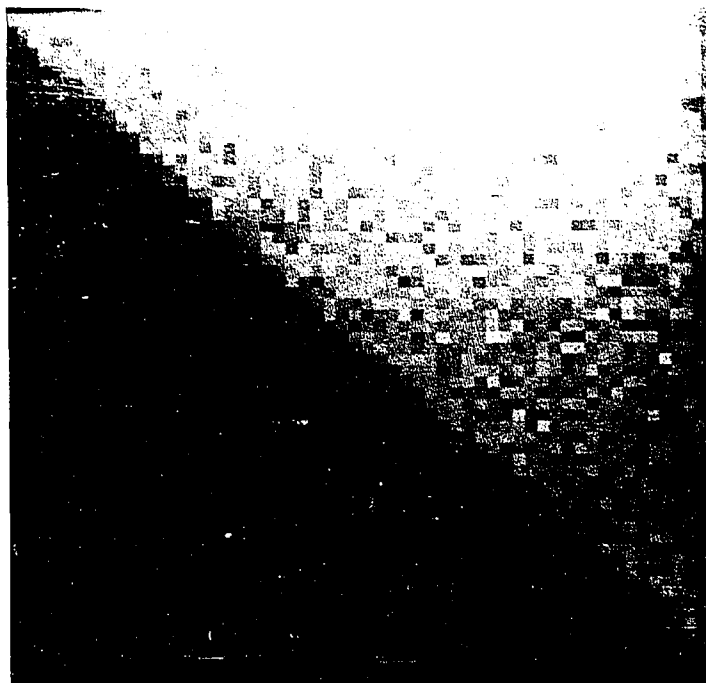
(b)

(c)

(d)

Figure 4-2. Images degraded with motion blur plus additive white noise ($\sigma^2 = 200$).

A second type of degradation is considered in order to make another comparison with previously published results. This degraded image is formed by simply adding white, Gaussian noise to the original image. The noise was again assumed to have zero mean and a standard deviation of 14.142. The result is shown in figure 4-3.

Figure 4-3.   Image degraded with additive white noise (σ^2 = 200).

The masking function is determined for each of the images in figure 4-2 according to step 1 of the algorithm. The values for k and r, the coefficients that determine the size of the neighborhood were both set equal to one. The masking values are then used according to equation (3-20) to determine the visibility function, which in turn is used to weight the variance of the noise in the Kalman filtering equations. An example of the masking function for figure 4-1b is shown in figure 4-4.

Figure 4.4.   Masking function for figure 4-2c with k=r=1.

Each of the images is divided into regions in step 2 of the algorithm. All of the images were divided into two regions in this step. In addition, figure 4-1b was also tested for the case in which it is divided into five regions. An example of the results of dividing figure 4-1c into two regions is shown in figure 4-5.
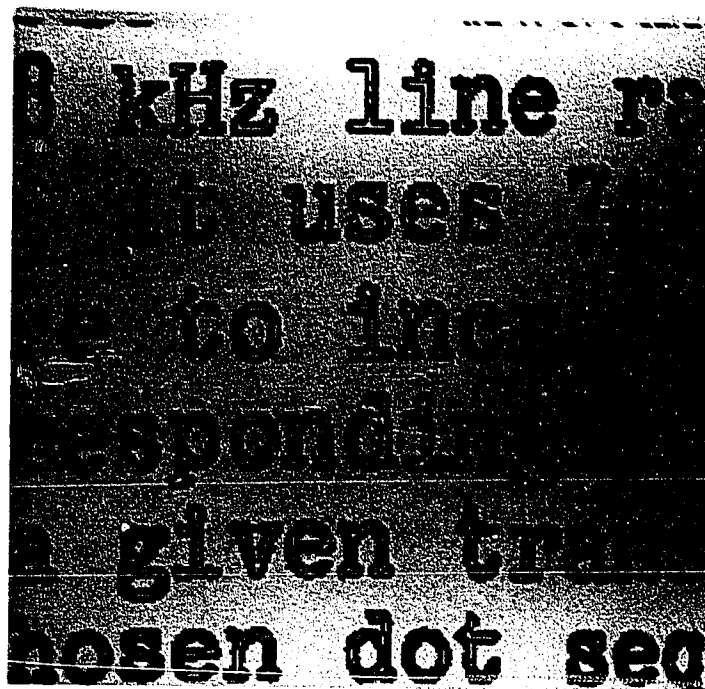
Figure 4-5.   Figure 4-2d divided into two regions.

The   results of determining the statistical information in step 3 of the algorithm are as follows:

Figure 4-1a: $R_1 = 1848.7 \exp(-.12|\tau| - .122|\sigma|)$,

Regions = 2 $R_2 = 1990.1 \exp(-.436|\tau| - .426|\sigma|)$.

Figure 4-1c: $R_1 = 2682.1 \exp(-.108|\tau| - .1609|\sigma|)$,

Regions = 5 $R_2 = 314.6 \exp(-.1994|\tau| - .3106|\sigma|)$,

$$R_3 = 393.53 \exp(-.4703|\tau| - .3826|\sigma|),$$

$$R_4 = 919.45 \exp(-.6512|\tau| - .6084|\sigma|),$$

$$R_5 = 1221.7 \exp(-.724|\tau| - .696|\sigma|),$$

Regions = 2 $R_1 = 2667.9 \exp(-.0973|\tau| - .0191|\sigma|),$

$$R_2 = 549.98 \exp(-.612|\tau| - .3954|\sigma|).$$

Figure 4-1d: $R_1 = 673.0 \exp(-.101|\tau| - .127|\sigma|),$

Regions = 2 $R_2 = 795.25 \exp(-.856|\tau| - .7012|\sigma|).$

From these autocorrelation functions the appropriate values were determined for the coefficient matrices A_p, B_p, c_p^T. The actual filtering procedure is now implemented and the results are presented in the next section.

II. Results

In order to compare the results of the adaptive nonlinear Kalman-type filtering algorithm with the existing state of the art, the results at several different stages of the filtering process are presented. A calculation of the average cummulative mean square error between the original image and the restored image was determined to give some quantitative assessment of the improvements. The error was determined as follows:

$$\text{Error} = \mathcal{E}^2 = \frac{1}{NM} \sum_{i=0}^{N-1} \sum_{j=0}^{M-1} [f(i,j) - \hat{f}(i,j)]^2, \qquad (4-17)$$

where N is equal to the array size in the horizontal direction and M is the array size in the vertical direction. For these images, N = M = 256.

Figure 4-6 shows the first stage in the restoration procedure. This is the implementation of the Aboutalib, et al. [2] algorithm. It should be noted that this figure demonstrates two of the problems that exist when an image has large differences in intensity levels. The filter does not respond as quickly as the intensity levels change and therefore the edges are not restored to their original sharpness. In addition, when there is a sudden change in intensity or there are poor initial conditions, a ringing is present while the filter attempts to adapt to the new conditions. The error that is present in this restored image is 3570.5.

Figure 4-7 is the result of adding to the first procedure the adjustment in the noise variance via the visibility function. As is expected the edges are sharper than those of figure 4-6. The error, however, has only been reduced. It is equal to 1994.55.

Figure 4-6. Restored image of figure 4-2c using the Aboutalib, et al. [1] algorithm.

Figure 4-7. Restored image of figure 4-2c using the visibility function.

The nonlinear adaptive Kalman-type filtering algorithm
is now implemented with the number of regions equal to two
and the result is shown in figure 4-8. The image is
improved and the overall error is reduced considerably to
795.24. The edges in figure 4-7 are still not as crisp as
one might hope for. An improvement is made by adjusting the
number of regions to a more nearly optimal number for this
image. The result of changing the number of regions from
two to five is shown in Figure 4-9. The edges in this
figure are crisper and the restored image does match the
original more closely as the error is now equal to 653.2.

Figure 4-8. Restored image of figure 4-2c using the
nonlinear adaptive Kalman-type filtering algorithm with the
number of regions equal to two.

Figure 4-9. Restored image of figure 4-2c using using the new algorithm with the number of regions equal to five.

The results of restoring figure 4-1d with the Aboutalib et al. [1] algorithm results in figure 4-10. The error is 1409.2. Now implementing the new restoration scheme on this image yields a restored image with an error equal to 725.95. The restored image is shown in figure 4-11.
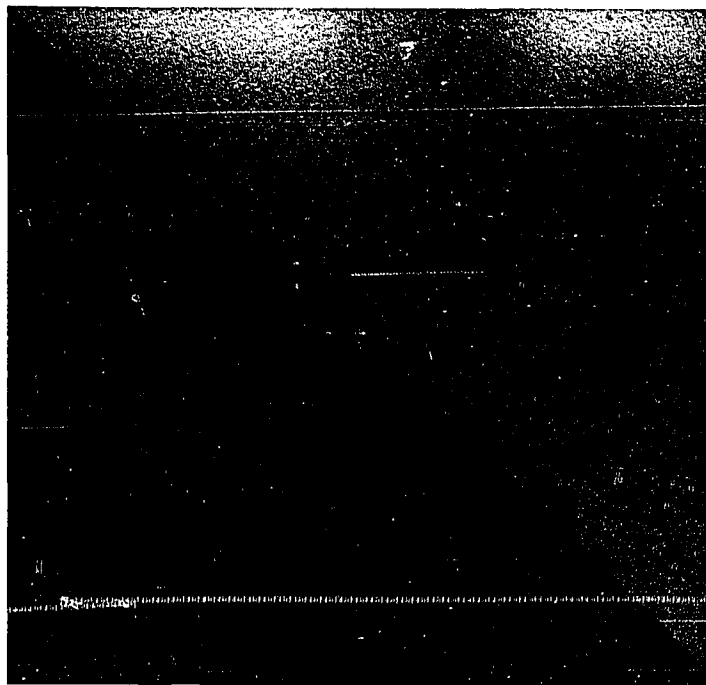
Figure 4-10.   Restored   image   of   figure   4-2d   using   the
Aboutalib, et al. [1] algorithm.

Figure   4-11.   Restored - image of figure 4-2d using the new
algorithm with the number of regions equal to two.

Finally, to get a better idea of what is actually resulting in the restored image at an edge, consider figure 4-12a and 4-12b. Figure 4-12a is the result of applying the nonlinear adaptive Kalman filtering algorithm to the distorted image in figure 4-2a. If we examine the zoomed configuration, it is seen that the edge has been improved, although it is still not perfect. The error for this case is 100.87.

(a)
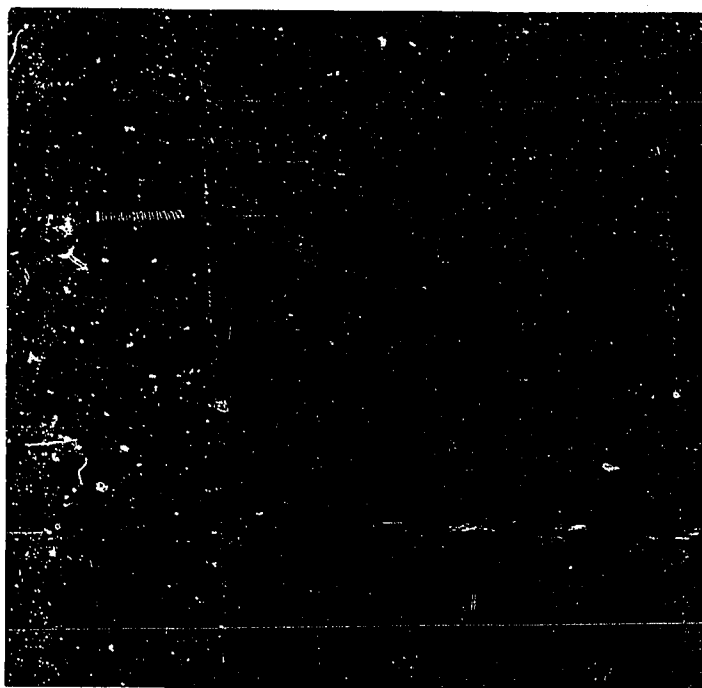
(b)

Figure4-12.   Restored image of figure   4-2a   using   the   new
algorithm   with   regions   equal   to   two.   Part   (b)   is   zoomed   by
a factor of four.

The   final   comparison   was   done   on   the   results   of
restoring   figure   4-3.   This   is   the   case   where   the   image   was
degraded   only   with   additive   noise.   Figure   4-13   shows   the
result   of   applying   the   restoring   filter   to   figure   4-3   if   it
includes   just   the   adaptation   to   the   noise   via   the   visibility
function.   The result is   fairly   noisy   and   the   edges   are
somewhat   blurred.   The   error   is   3534. 5.   The   result   of

restoring this same image with the adaptive nonlinear
Kalman-type filter is shown in figure 4-14. The image was
divided into five regions for this test and the resulting
error was 837.01.

Figure 4-13. Restored image of figure 4-3 with the
visibility function.

Figure 4-14. Restored image of figure 4-3 with the new algorithem and the number of regions equal to five.

CHAPTER 5

CONCLUDING REMARKS

A new recursive technique is presented in this dissertation for the restoration of images degraded by general image formation distortions and additive white noise. A vector difference equation model is used to represent the degradation in the image formation system. This type of description is easily adapted to a variety of applications where degradation occurs. The difference equation coefficient matrices [A, B, $\underline{c}^T$, $\underline{d}^T$] can be either constant or space-variant. Difference equation models are also used to characterize the object plane distribution function. The object plane is partitioned into regions based on the amount of spatial activity in the image.

It is shown that each of the regions can be uniquely characterized by the second order statistics of the region. The object plane distribution function $f_p(i,j)$ for the pth region is generated at the output of a linear system whose impulse response is determined by the autocorrelation function characterizing the region. The input to this system is a Gaussian, white noise source.

The above two difference equation models are combined to form a composite system of difference equations for each region. Recursive estimation techniques are applied to these composite difference equation models and the result is

a nonlinear adaptive Kalman-type filter described by the equations

$$\underline{w}_p(i,j|j) = [I - \underline{g}_p(j)\underline{c}_p]A_p\underline{w}_p(i*,j*|j*)$$
$$+ \underline{g}_p(j)g(i,j), \tag{5-1}$$

$$\underline{g}_p(j) = P_p(j)\underline{c}_p[\underline{c}_pP_p(j)\underline{c}_p + \sigma] , \tag{5-2}$$

$$P_p(j+1) = A_p[I - \underline{g}_p(j)\underline{c}_p]P_p(j)A_p + B_pR_pB_p, \tag{5-3}$$

for $p = 1,2,\ldots,k$, $\underline{w}(i,j|j)$ is the state vector, and A_p, B_p, R_p, $\underline{c}_p^T$ are the coefficient matrices specified by the image formation system degradation and the statistics of the input object plane distribution function. The variance of the additive noise is represented by σ^2 and $P_p(j)$ is the estimation error covariance matrix.

If the images to be restored are to be used by human observers it is desirable to account for the human visual system as part of the receiver characteristics. This is accomplished by weighting the statistics of the additive white noise by a visibility function. The visibility function is a subjective measure of the visibility of additive noise in an image by the human visual system. The variance of the observation noise σ^2 is adjusted at each pixel during the implementation of the filter making the scheme nonlinear in each region.

Two additional features are added to the adaptive nonlinear Kalman-type filter to account for inadequacies in the implementation phase. It is shown that it is not always

desirable to choose the state vector of pixel (i,j-1) as the previous state vector for pixel (i,j). A nearest neighbor criterion is proposed to determine which one of the state vectors of a previously processed pixel should be used as the previous state vector.

Finally, if there is insufficient information about the initial conditions for the state vector $\hat{\underline{w}}_p(i,j)$ or the error covariance matrix $P_p(j)$, an interpolation scheme is proposed to improve the estimates of the first points in a region. In summary, the adaptive nonlinear Kalman-type filtering scheme developed in the present work offers four primary improvements:

(1). The use of the visibility function to incorporate the properties of the human visual system as receiver characteristics.

(2). Partitioning of the image to allow for more accurate modeling of the second order statistics of the object plane distribution function.

(3). A nearest neighbor algorithm is utilized to determine the best previous state at the boundaries and in regions of high spatial activity.

(4). An interpolation scheme is provided for the improvement of initial condition information.

Implementation of this adaptive nonlinear Kalman-type filtering scheme was successful. Three types of images were used in the testing procedure, a simple geometric figure,

the face of a woman, and the image of a written text.

The cumulative mean square error, $\mathcal{E}$, calculated for the images restored·by the adaptive nonlinear Kalman—type filter showed improvement over the images restored by the previous recursive retoration schemes. Employing such an algorithm on the degraded image of figure 4-2c yields a value of 59.25 per pixel for $\mathcal{E}$. The restoration of this same image using the new adaptive nonlinear Kalman—type filter with the number of regions equal to two yields 28.2 per pixel for $\mathcal{E}$. Changing the number of regions to five reduced the error to 25.5 per pixel for $\mathcal{E}$.

The result of restoring the image of written text in figure 4-2d with the new filter is also encouraging; the error is 26.9 per pixel. The lowest error is seen in the restored image of the simple geometric image in figure 4-12a. The error was only 10 per pixel. This is to be expected as there is very little spatial activity in the image.

It is apparent from these results that this method of image restoration provides encouraging results. It also produces a general formulation so that it is easily adapted to a large variety of images.

Bibliography

1. Aboutalib, A., M.S. Murphy, and L.M.Silverman, "Digital Restoration of Images Degraded by General Motion Blurs," IEEE T. on Automatic Control, AC-22(3):294-302, June 1977.

2. Anderson, G.L., and A.N. Netravali, "Image Restoration Based on a Subjective Criterion," IEEE T. on Systems, Man and Cybernetics, CMS-6(12):845-853, December 1976.

3. Andrews, H.C., "Digital Image Restoration: A Survey," Computer, 7(5):36-45, May 1974.

4. Andrews, H.C., and B.R. Hunt, Digital Image Restoration, New Jersey:Prentice-Hall, 1977.

5. Budrikis, Z.L., "Visual Fidelity Criterion and Modeling," Proc. IEEE, 60(7):771-779, July 1972.

6. Cannon, T.M., "Digital Image Deblurring by Nonlinear Homomorphic Filtering," Ph.D. thesis, Computer Science Department, University of Utah, Salt Lake City, Utah, 1974.

7. Cole, E.R., "The Removal of Unknown Image Blurs by Homomorphic Filtering," Ph.D. thesis, Department of Electrical Engineering, University of Utah, Salt Lake City, Utah, 1973.

8. Ekstrom, M.P., "Numerical Image Restoration by the Method of Singular-Value Decompostion," Proc. Seventh Hawaii Intl. Conf. on Systems Science, Honolulu, Hawaii, 13-15, January 1974.

9. Franks, L.E., "A Model for the Random Video Process", BSTJ, 45(4):609-630, April 1966.

10. Frieden, B.R., "Restoring with Maximum Likelihood and Maximum Entropy," JOSA, 62(4):511-518, April 1972.

11. Frieden, B.R., "Image Restoration by Discrete Deconvolution of Minimal Length," JOSA, 64(5):682-686, May 1974.

12. Frieden, B.R., and J.J. Burke, "Restoring with Maximum Entropy II: Superresolution of Photographs of Diffraction-Blurred Images," JOSA, 62(10):1201-1210, October 1972.

13. Goldmark, P.C., and J.M. Hollywood, "A New Technique for improving the Sharpness of Television Pictures," Proc. IRE, 39:1314-1322, 1951.

14. Graham, R.E., "Snow Removal — a Noise-Stripping Process for Picture Signals," IRE T. on Information Theory, IT-8:129-144, October, 1962.

15. Gray, R.M., "Toeplitz and Circulant Matrices: A Review," Report SU-SEL-71-032; Stanford Univ., California, 1971.

16. Habibi, A., "Two-Dimensional Bayesian Estimate of Images," IEEE Proc. 60(7):878-883, July 1972.

17. Harris, J.L., "Image Evaluation and Restoration," JOSA, 56(5):569-574, May 1966.

18. Helstrom, C.W., "Image Restoration by the Method of Least Squares," JOSA, 57(3):297-303, March 1967.

19. Huang, T.S., "Image Enhancement: A Review," Opto-Electronic., 1:49-59, 1969.

20. Huang, T.S.; W.F. Schrieber; O.J. Tretiak, "Image Processing," Proc: IEEE, 59(11):1586-1608, November 1971.

21. Hunt, B.R., "The Application of Constrained Least Squares Estimation to Image Restoration by Digital Computer," IEEE T. on Computers, C-22(9):805-812, September 1973.

22. Hunt, B.R., "Digital Image Processing," Proc. IEEE, 63(4):693-708, April 1975.

23. Hunt, B.R., "Bayesian Methods in Nonlinear Digital Image Restoration," IEEE T. on Computers, C-26(3):219-229, March 1977.

24. Hunt, B.R., and H.J. Trussell, "Recent Data on Image Enhancement Programs," Proc. IEEE, 61(4):466, April 1973.

25. Jain, A.K., "A Semicausal Model for Recursive Filtering of Two-Dimensional Images," IEEE T. on Computers, 26(4):343-350, April 1977.

26. Johnston, E.G., and A. Rosenfeld, "Geometrical
        Operations on Digitized Pictures," in Picture
        Processing and Psychopictorics, (B.S. Lipkin and
        A. Rosenfeld, eds.), pp. 217-240, New York:
        Academic Press, 1970.

27. Keshavan, H.R., and M.D. Srinath, "Interpolative Models
        in Restoration and Enhancement of Noisy
        Images," IEEE T. on Acoustics, Speech, and
        Signal Processing, 25(6):525-534, December 1977.

28. Kondo, K, Y. Ichioka, and T. Suzuki, "Image Restoration
        by Wiener Filtering in the Presence of Signal
        Dependent-Noise," Applied Optics, 16(9):2554-2558,
        September 1977.

29. Kovasznay, L.S.G., and H.M. Joseph, "Image
        Processing," Proc. IRE. 43:560-570, 1955.

30. Krishnamurthy, E.V., "Recursive Computation of the
        Pseudo-Inverse for Applicaions in Image
        Restoration and Filtering,"Univ. of Maryland,
        Computer Sciences Tech. Report Series - 580,
        September 1977.

31. Levi, L., "On Image Evaluation and Enhancement,"
        Opt. Acta, 17(1):59-76, January 1970.

32. Limb, J.O., and C.B. Rubenstein, "On the
        Design of Quantizers for DPCM Coders: A
        Functional Relationship Between Visibility,
        Probability and Masking," IEEE T. on
        Communications, COM-26(5):573-578, May 1978.

33. MacAdam, D.P., "Digital Image Restoration by
        Constrained Deconvolution," JOSA, 60(12):
        1617-1627, December 1970.

34. Martelli, A., and U. Montanari, "Optimal Smoothing in
        Picture Processing: An Application to
        Fingerprints," Proc. IFIP Congr., Booklet
        TA-2, 86-90, 1971.

35. Merserau, R., and D. Dudgeon, "Two-Dimensional Digital
        Filter," Proc. IEEE, 63(4):610-623, April 1975.

36. Nahi, N.E., Estimation Theory and Application,
        New York:R.E. Krieger Publishing Co., 1976.

37. Nahi, N.E., and T. Assefi, "Bayesian Recursive
        Image Estimation," IEEE T. on Computers,
        C-21(7):734-738, July 1972.

38. Nahi, N. E. , and C. A. Franco, "Recursive Image
    Enhancement - Vector Processing," IEEE T. on
    Communications, COM-21(4):305-311, April 1973.

39. Netravali, A. N. , and B. Prasada, "Adaptive Quantization
    of Picture Signals Based on Spatial Masking,"
    Proc. IEEE, 65(4):536-548, April 1975.

40. O'Handley, D. A. , and W. B. Green, "Recent
    Developments in Digital Image Processing at the
    Image Processing Laboratory at the Jet Propulsion
    Laboratory," Proc. IEEE, 60(7):821-828, July 1972.

41. Oppenheim, A. V. , R. W. Schafer, and T. G. Stockjam, Jr.,
    "Nonlinear Filtering of Multiplied and Convolved
    Signals," Proc. IEEE, 56(8):1264-1291,
    August 1968.

42. Phillips, D. L. , "A Technique for the Numerical
    Solution of Certain Integral Equations of the
    First Kind," J. ACM, 9:84-97, 1962.

43. Polak, E. , Computational Methods in Optimization,
    New York:Academic Press, 1971.

44. Prewitt, J. M. S. , "Object Enhancement and Extraction,"
    in Picture Processing and Pschopictorics,
    (B. S. Lipkin and A. Rosenfeld, eds.), pp. 75-149,
    New York:Academic Press, 1970.

45. Richardson, W. H. , "Bayesian-Based Iterative Method
    of Image Restoration," JOSA, 62(1):55-59,
    January 1972.

46. Robbins, G. M. , and T. S. Huang, "Inverse Filtering for
    Linear Shift-Variant Imaging Systems," Proc. IEEE,
    60(7):862-872, July 1972.

47. Roetling, P. G. , "Image Enhancement by Noise
    Suppression," JOSA, 60(6):867-869, June 1970.

48. Rosenfeld, A. , and A. C. Kak, Digital Image Processing,
    New York:Academic Press, 1976.

49. Rubenstein, C. B. , and J. O. Limb, "On the
    Design of Quantizers for DPCM Coders: Influence
    of the Subjective Testing Methodology," IEEE T.
    on Communications, COM-26(5):565-572,
    May 1978.

50. Sawchuk, A. A. , "Space-Variant Image Motion
    Degradations and Restoration," Proc. IEEE,
    60(7):854-861, July 1972.

51. Sawchuk, A.A., "Space-Varaint System Analysis
        of Image Motion," JOSA, 63(9):1052-1063,
        September 1973.

52. Sawchuk, A.A., "Space-Variant Image Restoration
        by Coordinate Transformation," JOSA,
        64(2):138-144, February 1974.

53. Slepian, D., Linear Least-Squares Filtering of Distorted
        Images," JOSA, 57(7):918-922, July 1967.

54. Stockham, T.G., Jr., "Image Processing in the
        Context of a Visual Model," Proc. IEEE,
        60(7):828-841, July 1972.

55. Stockham, T.G., Jr., R. Ingebretsen, and T.M. Cannon,
        "Blind Deconvolution by Digital Signal
        Processing," Proc. IEEE, 63(4):679-692,
        April 1975.

56. Thiry, H., "Some Qualitive and Quantitive results on
        Spatial Filtering of Granularity," Applied Optics,
        3:39-43, 1964.

57. Troy, E.B., E.S. Deutsch, and A. Rosenfeld, "Gray-Level
        Manipulation Experiments for Texture Analysis,"
        IEEE T. on Systems, Man, and Cybernetics,
        SMC-3(1):91-98, January 1973.

58. Twomey, S., "On the Numerical Solution of
        Fredolm Integral Equations of the First Kind by
        the Inversion of the Linear System Produced by
        Quadrature," J. ACM, 10:97-101, 1963.

59. Twomey, S., "The Application of Numerical Filtering
        to the solution of Integral Equations Encountered
        in Indirect Sensing Measurements," J. Franklin
        Inst., 297:95-109, 1965.

60. Woods, J.W., and C.H. Radewan, "Kalman Filtering in
        Two-Dimensions," IEEE T. on Information
        Theory, IT-23(4):473-482, July 1077.